MONITORING AND ANALYZING OF DESERTIFICATION TREND IN NORTH SUDAN USING MODIS IMAGES FROM 2000 to 2014

By

Tarig Adil Mohamed

B.Sc., Future University

A thesis
Submitted in Partial Fulfillment of the Requirements for the
Master of Science degree

Department of Geography and Environmental Resources
in the Graduate School
Southern Illinois University Carbondale
December 2016

THESIS APPROVAL

MONITORING AND ANALYZING OF DESERTIFICATION TREND IN NORTH SUDAN USING MODIS IMAGES FROM 2000 TO 2014

By

Tarig Adil Mohamed

A Thesis Submitted in Partial

Fulfillment of the Requirements

for the Degree of

Master of Science

in the field of Geography and Environmental resources

Approved by:

Dr. Guangxing Wang, Chair
Dr. Justin Schoof
Dr. Leslie Duram

Graduate School
Southern Illinois University Carbondale
5/12/2016

AN ABSTRACT OF THE THESIS OF

Tarig Adil Mohamed, for the Master of Science degree in GEOGRAPHY AND ENVIROMNTAL RESORCES, presented on 12th May 2016, at Southern Illinois University Carbondale

TITLE: MONITORING AND ANALYZING OF DESERTIFICATION TREND IN NORTH SUDAN USING MODIS IMAGES FROM 2000 TO 2014

MAJOR PROFESSOR: DR. Guangxing Wang

Desertification is a serious threat that damages the environment in many African countries, as a result of climatic factors and population growth. This research, investigated and monitored the dynamics of the desert area in the Republic of Sudan using geographic information system (GIS) and remote sensing images. The expansion of desertification in Sudan, particularly in Darfur, Kordofan, and Alshymalia states has, increased rapidly. Many efforts have been committed to understanding its dynamics, causes, and impacts. However, the data are still lacking. In this study Moderate-resolution Imaging Spectroradiometer (MODIS) Normalized Different Vegetation Index (NDVI), Enhanced Vegetation Index (EVI), and Gross Primary Productivity (GPP) images were acquired for the months of July, August, and September (growing seasons of the vegetation in the study area) of the years 2000, 2009, and 2014 respectively. Landsat 8 Operational Land Imager (OLI) data were used to compare and validate the result of MODIS data. Artificial Neural Network (ANN) and Spectral Mixture Analysis (SMA) techniques were utilized to produce three classification maps, and to address the issue of the mixed pixel. Post-classification change detection method was used to quantify the change that had occurred in the study area. The results show that the overall classification accuracy for the MODIS data for the year 2000, 2009, and 2014 was 79.52 %, 81.90 %, and 85.76 %

respectively, and there was a significant increase in the expansion of the desert area towards the south and southwest of the study area. The temporal period between 2000 and 2009 indicated the greatest conversion of vegetation to desert area. Population growth and climatic changes such as temperature increment and precipitation variation were the major factors that led to the desert expansion. The result of this study will provide the people of Sudan with the information regarding desert area land expansion during the past 14 years, thereby raising awareness about the environmental problem in Sudan.

DEDICATION

To my father Adil Abdallah, from whom I have got to learn how life is

To my mother Hanan Haroun, from whom I have got to know how love is

To my professor Dr. Guangxing Wang, from whom I have got to know how learn is

I dedicate this work with a great love and respect

ACKNOWLEDGMENTS

I would like to express my special gratitude to my advisor Dr. Guangxing Wang for his support and motivation. His knowledge and experience guided me in all facets in this research as well as giving me the opportunity to grow my knowledge in the GIS and remote sensing field. I would also like to thank my thesis committee: Dr. Justin Schoof and Dr. Leslie Duram for taking the time to read my thesis and for the helpful response. Finally, I would like to thank all of my friends in the Geography Department for their help and support.

TABLE OF CONTENTS

LIST OF TABLES

TABLE PAGE

LIST OF FIGURES

FIGURE PAGE

LIST OF ABBREVIATIONS

Artificial neural network	(ANN)
Enhance Vegetation Index	(EVI)
Enhanced Thematic Mapper	(ETM+)
Global Positioning System	(GPS)
Gross Primary Productivity	(GPP)
Ground Control Point	(GCPs)
Land Use and Land Cover	(LULC)
Landsat Multispectral Scanner	(MSS)
Landsat Thematic Mapper plus	(TM+)
Moderate-resolution Imaging Spectroradiometer	(MODIS)
MODIS Re-projection Tool	(MRT)
Multi-layer Perceptron	(MLP)
Normalization Difference Vegetation Index	(NDVI)
Root Mean Square Error	(RMSE)
Royal Jordanian Geographic Center	(RJGC)
Spectral Mixture Analysis	(SMA)
United Nation Convention to Combat Desertification	(UNCCD)
United Nation Environment Program	(UNEP)
Universal Traverse Mercator projection system	(UTM)
Vegetation Cover Conversion	(VCC)

CHAPTER 1

INTRODUCTION

Desertification is a type of land degradation that deteriorates the environment and threatens life on earth's surface. Currently, desert and semi-desert areas occupy around 25.5 million km², which represents approximately 40% of the world's land (Hulme, 1996). Due to increasing global population, anthropogenic activities, global warming and climate change, desertification is continuing to expand at a rapid pace. It also has a great impact on ecosystems in many parts of the world. Consequently, desertification has become a major concern in the world today. Desertification is also one of the major environmental problems in Sudan, which is considered one of the most arid territories in Africa (Ayoub, 1997).

In Sudan, about 31% of the country's land is hyper-arid, and 63% is dry lands at risk of desertification (Ayoub, 1997). This dry land, where most of the country's population lives, is negatively affecting the economic development and quality of life of the Sudanese society. The major reasons for desertification in this region include drought, population growth, intensive agriculture, deforestation, rapid urbanization, civil war, and deterioration of the economy, all of which have reduced agriculture production and local farming. Initiatives to address desertification expansion must include improved cultivation methods, proper grazing management, reforestation, and improving crop production systems. It is important to quantify the expansion of desert areas in Sudan in order to explore the causes and to identify appropriate methods in order to mitigate and address desertification (Laki, 1994).

1.1 **Research Statement**

The objective of this study is to quantify Sudan's desert areas and their dynamics and to investigate the different impacts of desertification expansion on land use and land cover (LULC), in Sudan using GIS and remote sensing based monitoring methodology for the years 2000 to 2014. Additionally, it also aims to examine the relationships between desertification expansion and population growth, climate change, and vegetation condition. Furthermore, it will not only provide the people of Sudan with information regarding desertification land expansion during the past 14 years, but will also raise awareness of the problem.

1.2 Research Questions and Hypotheses

This study answered the following research questions with corresponding hypotheses to be tested.

Research Question One:

1) How has the desert area in Sudan developed spatially and temporally?

Research Hypothesis One:

The desert area in Sudan has continuously expanded over the past years 2000 to 2014.

Research Question Two:

2) What are the major factors that have significantly affected the spatial and temporal expansion of the desert areas in Sudan?

Research Hypothesis Two:

Population growth and global climate change are the most important factors speeding up the expansion of desert areas in Sudan.

Research Question Three:

3) What are the impacts of desertification on the environment and vegetation conditions in the past and present?

Research hypothesis Three:

Desertification has caused the loss of water and vegetation, and decreased productivity of land.

1.3 Significance of the Study

- In Sudan, desertification has been a serious issue in recent history due to the conversion of a large areas of productive land into nonproductive land. Despite the early awareness about desertification in Sudan, few serious actions have been taken to combat desertification.
- This study will provide a quantification of the desert area in Sudan and information about LULC changes for the years 2000 to 2014.
- This study is highly significant in that it will increase awareness and knowledge regarding desertification in Sudan. Additionally, it will provide insight of the main factors that drive desertification expansion in Sudan.

CHAPTER 2

LITERATURE REVIEW

2.1 Desertification

The term desertification has been defined by the United Nation Convention to Combat Desertification (UNCCD) as the "process that leads to the aridity of soil and land and thus to the loss of water and reduction of vegetation, wildlife, and capacity for livestock" (UNCOD, 1977). A second definition provided by UNCODH/ CONF (1977) states that desertification is the degradation of biological capabilities of the land; and can eventually give rise to desert conditions. Desertification refers to the deterioration of dry land, where there is less precipitation than is demanded in an area (Kassas, 1995). Lastly, the United Nations Environment Program (UNEP) has defined desertification as the diminution or destruction of arid, semi- arid and dry sub-humid areas as a consequence of anthropogenic activities.

Land degradation refers to the transformation of productive land such as farmland, into non-fertile land such as desert areas (Kassas, 1995). Degradation in farmland is usually due to large scale irrigation system and sterile drainage (Kassas, 1995). Symptoms of land degradation are various in different land use structures such as the reduction in rangelands productivity because of decreased bio-productivity and soil nutrition (Kassas et al., 1991). The most prominent symptom of degradation is desertification. According to the world Atlas of desertification (UNEP, 1992), dry lands are divided into four categories: Hyper- arid, arid, semi-arid and dry sub-humid. Table 1 provides a summary of dry land areas in the world.

Table 1: *World dry lands in millions of hectares (ha) (UNEP/GRID, 1991).*

	Africa	Asia	Australia	Europe	North America	South America	World total	% (ha)
Hyper-arid	672	277	0	0	3	26	978	16
Arid	504	626	303	11	82	45	1571	26
Semi-arid	514	693	309	105	419	265	2305	37
Dry sub-humid	269	353	51	184	232	207	1296	21
Total	1959	1949	663	300	736	543	6150	100

Globally, dry land occupies approximately 40% of earth's land surface (Hulme, 1996). Many of the residents residing on dry lands are living in low income countries, which explains the 400,000 deaths per year worldwide as a result of drought and flood (OFDA, 1990). Desert areas continue to sprawl and the consequent negative effects persist (UNEP, 1992).

2.2 Causes and Impacts of Desertification

Global climate change is one of the most significant factors leading to desertification. Climate change is typically characterized by the increase of temperature, reduction of rainfall, and considerable variation in both temperature and rainfall, all of which decrease the amount of water available for vegetation growth; and increases the likelihood of drought (Kassas, 1995). Increasing population and anthropogenic activities, such as over-farming, overgrazing, deforestation, and inadequate irrigation have had significant impacts on desertification expansion (Ouma and Ogallo, 2007). Bath (1999) provided a study in monitoring desertification in Saudi Arabia, and concluded that continued grazing decreases the value of rangelands. Socioeconomic

impacts of desertification include increasing the poverty level of the community and destroying natural and economical resources (Ouma and Ogallo, 2007).

2.3 Desertification in Africa and Sudan

The Sahara desert in Africa is one of the largest desert areas in the world and extends from the Atlantic Ocean in the west to the Red Sea in the east. Desertification threatens approximately 43% of the total land in Africa (UN, 2006). During the past 30 years, Africa's population has doubled to 400 million, which has negatively impacted natural resources (Ouma and Ogallo, 2007). According to Reich et al. (2001) roughly 2.5 million km² of the total land is currently under a low risk, 3.6 million km² under a medium risk, 4.6 million km² under a high risk, and 2.9 million km² under an extremely high likelihood of desertification.

The Republic of Sudan has an area that is approximately double that of Great Britain (Fouad and Ibrahim, 1978). Sudan is the biggest country in Africa covering an area of 2.5 million square kilometers. Desertification is one of the major issues threating Sudan and resulting in destruction of natural resources and agricultural land. Sudan contains four desert areas: 1) Bayuda desert located in the north of Khartoum, Sudan and south of the Nubian Desert. 2) Nubian Desert located in the eastern area of Sahara desert between the Nile River and the Red Sea. 3) Libyan Desert located in the north of Sudan 4) Eastern Desert is a portion of the Sahara Desert. Based on a soil erosion index developed by Kennedy-Cooke (1944), degradation of soil and vegetation is progressing at a fast space and expanding rapidly in the portion of the Red Sea Hills which will become a serious problem in the future. Human factors have led to soil degradation of 75 million ha (Ayoub, 1997). According to the Global Assessment of Human-induced Degradation (GLASOD), regions of severe and very severe degradation currently

occupy 58 million ha in Sudan. Ayoub (1997), investigated various factors of soil erosion and found that overgrazing was the primary cause, followed by rain-fed agriculture, deforestation for firewood purposes, and overuse of vegetation, accounting for about 47%, 22%, 19% and 13% of soil eroded land respectively.

2.4 Desertification Change Detection Using Remote Sensing

Remote Sensing has been widely used to detect and quantify desertification and its expansion. Remotely sensed data includes aerial photographs and satellite images, such as high spatial resolution QuickBird images, medium spatial resolution Landsat and SPOT satellite images, and coarse spatial resolution (MODIS) images. Selection of remotely sensed images greatly depends on the requirements of the information needed at different spatial resolutions, its accuracy, and availability of budget.

Bakri et al. (2001) conducted a study to monitor transition zones using aerial photographs and satellite imagery. The Royal Jordanian Geographic Center (RJGC) combined black and white aerial photographic and topographic maps at scale 1:25 000 and 1:50 000 to detect desertification expansion. Hard copy geo- corrected satellite imagery was used to assist and validate the interpretation. They found that the study area has 30-50% higher vegetation cover and 0-5% lower vegetation cover in another area due to overgrazing and human activity (Bakri et at., 2001).

Another significant study conducted by Ares et al. (2003) aimed to discover the early stages of dry land degeneration and to quantify desertification at large scales using aerial photographs (×36 exposures). The photos were taken at an altitude of 660 m from the ground to achieve nadir-oriented exposures. Landsat Thematic Mapper ™ was acquired and used to

perform geo-rectification for each image. The image digitizing processes includes: modifying the negative exposure films (Kodak color film 1002-7, Buenos Aires, Argentina) to hard copies (150.2× 101.0 mm), and then digitizing the copies into gray palette (binary eight but byte $^{-1}$ integers, digital values: 0-255) with a desk page scanner (Umax- Astra 3400 Fremont CA, USA) at a resolution of 75, 150, 300 and 600 dpi (Ares et al., 2003). The images were tested for sub-saturated value histogram to eliminate information loss. They found that the early stages of anthropogenic driven dryland degeneration was first uncoupling of spatial vegetation pattern from those of runoff at a landscape scale, and a progressive coupling to the spatial pattern of the wind regime (Ares et al., 2003).

Another study conducted by Huang and Siegert (2006) aimed to detect the areas at risk of desertification in North China using SPOT VEGETATION images. The data contained four spectral bands (blue, red, NIR, MIR), four view geometrics angles (VZA, VAA, SZA, SAA), and one Status Map (SM). Cloud and snow were removed using the information in the bands SM. However, MIR strips were selected and removed using an average 7×7 filter. NDVI were acquired with a formula of (b3- b2)/ (b3+ b2) where b3 is NIR and B2 is Red. They found that 1.60 million km² of area was at risk of desertification, and concluded that SPOT-VEGETATION imagery was very helpful to discover large-scale dynamics of environmental change and desertification process (Huang and Siegert, 2006).

The expansion of the sand sheet and dunes, representing the existence of Aeolian desertification, can be observed in remote sensing images (Liu, 1996). Hu et al. (2012) aimed to monitor the expansion of Aeolian decertified land (ADL) in the area of Yangtze River by using remote sensing and geographic information system (GIS) for four years (1975, 1999, 2000, and 2005). Hu et al. (2012) used Landsat Multispectral Scanner (MSS) images for 1975, Thematic

Mapper^{TM} images for 1990, and Enhanced Thematic Mapper (ETM+) images for both 2000 and 2005. They conducted image geo-referencing using 40 ground control points (GCPs), the root means square error of the geometric correction between two images was restricted to one or two pixels. The nearest neighbor method was used to resample the image to a spatial resolution of 30 m×30 m (Hu et al., 2011). They found that in 2005 the area of Aeolian desertification land was 33,189.70 km² accounting for 23% of the total land area in the source region of the Yangtze River, between 1975 and 2005, the area of Aeolian desertification grew by 2,678.43 km².

Wang et al. (2012) did a similar study in the same region for four years (1975, 1990, 2000, and 2010) and classified the intensity of Aeolian desertification into four classes (slight, moderate, severe, and extremely severe). The result of the study revealed an ADL area of 47,833 km² in 2010, implying a significant increase in rate. It increased by 2,228 km² (4.67 %) between 1975 and 1990. A portion of the ADL has been rehabilitated and thus, the area of ADL has since decreased by 930 km² from 1990 to 2000 (1.86%), and by 1,223 km² from 2000 to 2010 (Wang et al., 2012).

The issue of land deterioration in the eastern province of Saudi Arabia is not a new phenomenon. According to Barth (1999), the main reason driving the reduction of vegetation is overgrazing and increasing sand motion. The study used Global Positioning System (GPS) to record the ground path, and a video camera to determine the vegetation cover using a Macintosh IIsi computer. The obtained images were categorized into vegetated and non-vegetated areas using ERDAS IMAGINE. Landsat TM images were used to identify differences in vegetation cover between 1984 and 1991, and ERDAS IMAGINE was used to carry out image processing. The study showed that the size of the dune field approximately doubled in 15 months (Barth, 1999).

Another significant study conducted by Shalaby and Tateishi (2006) aimed to identify LULC changes in the Northwestern coasted zone of Egypt. Landsat TM and ETM+ images dated May 20 of 2001 and June 7 of 1987 were acquired and used. The geometric correction was accomplished using GCPs from topographic maps produced in 1983 with a scale of 1:5000. Supervised classification was carried out based on ground checkpoint and digital topographic maps of the study area. The result showed that due to agriculture and tourism growth, there was an increase in the vegetation degradation and water logging (Shalaby and Tateishi, 2006).

Abd El-Kawy et al. (2011) used the same methodology to monitor LULC changes in Western Nile Delta of Egypt. In this study, a supervised classification was used to complete classification of four Landsat images for the years 1984, 1999, 2005, and 2009. The study showed that about 28%, 14%, and 9% of the barren land was converted into agriculture land respectively (Abd El- Kawy et al., 2011).

Using Landsat MSS, TM, and ETM+ data, Dewan and Yamaguchi (2009) assessed LULC changes and urban development in Dhaka, Bangladesh. The geometric correction was carried out using 1997's Landsat TM images as a reference. More than 45 GCPs were used to geo-reference the 1997's image to the Bangladesh Transverse Mercator (BTM) system (Dewan and Yamaguchi, 2009). Anderson Scheme level I method was used to classify LULC types in this study (Anderson et al., 1976). To evaluate the classification and create error matrix (Congalton, 1991) a total of 125 unsystematic pixels were collected. The outcome of this study represented a significant reduction in the areas of water bodies, cultivated land, vegetation, and wetland and an increase of urban land due to population growth; and economic development (Dewan and Yamaguchi, 2009).

Qiong et al. (2006) monitored and predicted land use change in Beijing using remote sensing and GIS for three time periods (1986, 1991, 1996, and 2001). The Anderson Scheme of land use classification was adopted (Anderson et al., 1976). Each of the Landsat images was geo-referenced to the Beijing local coordinate system on a 1:50,000 scale topographic map. The nearest neighbor algorithm was used to keep the original brightness value of the pixel without change. The radiometric correction was used to discover the change of surface reflectance. The maximum likelihood method was applied for land use classification. Four bands of TM were used for gathering and processing training site data by mean of on- screen section of the polygon training method. The results indicated that there was a rapid change in urban growth and degradation of crop land between 1986 and 2001 (Qiong et al., 2006).

Xiao et al. (2004) provided a study aiming to monitor urban expansion and land use change in Shijiazhuang, China, using remote sensing and GIS. Landsat TM image and ETM+ image were collected in 1987 and 2001, respectively. TM images were geometrically corrected to the Universal Traverse Mercator projection system. ETM+ image were geo- referenced and matched to the TM image with the total RMS error of less than half a pixel. The supervised classification method was used to complete classification of Landsat images. The result showed that the urban area of Shijiazhuang city expanded from 6.31 km² in 1934 to 165.5 km² in 2001 with an average rate of 2.4 km² per year (Xiao et al., 2004).

Xu et al. (2009) evaluated desertification in Ordos Plateau, China, using remote sensing for three time periods (1980, 1990, and 2000). They used Landsat MSS images for 1980, TM images for 1900, and ETM+ images for 2000. Each of the images was geo-referenced to the WGS_1984_ UTM projection coordinate system. The desert area was divided into five categories namely non-desert, low desert, medium desert, high desert, and extreme desert. A

decision tree was used for classification. They found that from 1990 to 2000 desertification decreased, while due to anthropogenic activities desertification increased from 1980 to 1990 (Xu et al., 2009).

Dubovy et al. (2012) investigated cropland degradation in Uzbekistan using raster data, MODIS images (MOD12Q1), vector data, a LULC map from 2001-2009 derived from 250 m MODIS data, and ancillary data, including groundwater table data for the year1990 and 2004. The method used was based on MODIS NDVI and spatial logistic regression modeling. They found that vegetation degradation was specifically concentrated on low productivity land, and the spatial pattern was mostly related to the level of the groundwater table (Dubovy et al., 2012).

Liu and Wang (2005) aimed to monitor desertification in arid and semi-arid regions in China using MODIS data. Five desertification indexes were selected for large- scale desertification monitoring (MSAVI, FVC, Albedo, LST, TVDI). Unsupervised classifier, maximum likelihood classifier, and decision tree were employed for this study. They found that the speed of desertification was faster than that of rehabilitating. Wessels et al. (2007) monitored relevance of rangeland degradation in semi-arid areas in northeastern South Africa using MODIS data. Degradation areas were estimated using the growing-season sum of NDVI. They found that degradation had a significant influence on long-term vegetation productivity, and overgrazing was the primary cause of land degradation. Zhan et al. (2002) used MODIS 250 m data to monitor land cover change in southern Brazil. Five datasets of MODIS level 1B 250 m data were generated, and decision trees classifier was applied in this study. The results showed that this methodology was suitable for monitoring Vegetation Cover Conversion (VCC).

Holcomb (2001) conducted an archeological survey in arid areas of the Gobi desert of southern Mongolia using Radarsat satellite with a moveable antenna to allow for data collection

at look angles of 10-59 degrees of nadir in all directions. A total of 20-30 tie- points were selected and used to decrease the Root Mean Square Error (RMSE). GPS were used to collect latitude/longitude information. The result showed that Paleolithic cultural artifacts have been successfully detected (Holcomb, 2001).

CHAPTER 3

MATERIALS AND METHODS

3.1 Physiography of the Study Area

The study area is located in the northwestern region of the Republic of Sudan (Figure 1), which is one of the twelve Sahara desert countries. The size of the study area is approximately 5,739,131 sq. kilometers and is located between 11º43' 00"N and 19º54' 41"N latitude and 024º 00' 57" E and 031º 41' 04" E longitude. The study area covers the rural states of Kordofan, Darfur, and a portion of the Alschamalya, all of which are considered as the driest states in Sudan (Figure 1). These states are bordered by South Sudan to the south, the Blue Nile in the east, the Central African Republic in the southwest, and Chad from the west.

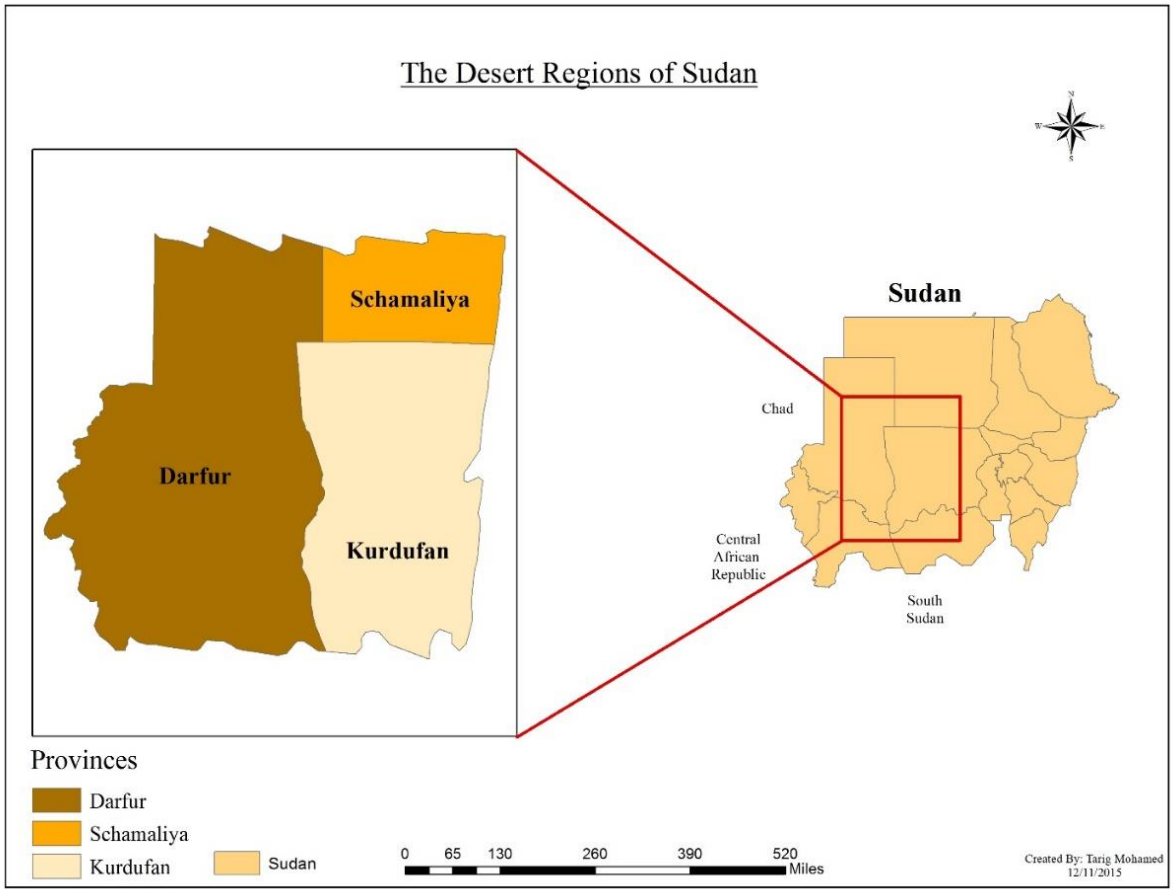

Figure 1: The driest provinces regions in Sudan.

The Republic of Sudan is divided into five arid zones: a hyper-arid zone that contains vegetation mainly during summer season; an arid zone containing grass that is a source of food for sheep, goats and camels and is characterized by high-speed wind associated with summer thunderstorms that lead to dust storms; a semi-arid zone that contains tall herbaceous plants and Acacia woodland, where agriculture is highly dependent on rain; a dry sub-humid zone; and a Moist Sub-humid zones which occupies 12 % of the total area of the country and it contains luxuriant vegetation. This zone is located near the border of the Democratic Republic of Congo and Central Africa Republic (Ayoub, 1997). The variability of climate, soil condition and topography with vegetation and diversity of contrast are shown in Table 2.

Table 2: *Regions of Sudan plants (Wickens, 1991).*

Region	Characteristics
Desert	Sandy soil, limited to the natural plant growth in seasonal creeks and the banks of the Nile
Sem-Desert	Occupied by Forklift plants, yearbook plants, seasonal pastures, and cultivation of rain.
Savanna Poor	Occupied by spine acacia trees, and hashab trees
Rich Savanna	Occupied by non-thorn tress, and it is rich pastures.
Region Dams	Occupied by rivier herbs.
Rainforest	Tropical forest

3.1.1 Population, climate, and elevation:

In 1960, the population of Sudan was estimated to be 7.5 million people. During the last five decades, the population of Sudan has increased by 415 percent and has grown to a population of 38.8 million in 2014. The total population of Sudan represents 0.5 % of the total

world population (http://www.tradingeconomics.com/). According to UNICEF, the population in the arid regions of Sudan was estimated at 10.5 million people. Sudan has a tropical climate, which is characterized by high temperatures most of the year (Figure 2). The climate is warm particularly during the dry, hot, and wet seasons (Elagib, 2010). During the dry season (March to April) the average daily air temperature is about 29 °C to 34 °C (Oliver, 2004). During the rainy summer season (July to August), temperature rangr from 31 °C to 32 °C. In winter, the average daily temperature is between 23 °C to 28 °C.

The majority of the precipitation in Sudan falls between July and August (Figure 3). Rainfall is limited to the summer season. Summer rains in western and southern Sudan have decreased by 10-20 percent since the 1970s. In the hyper-arid region, the annual rainfall is about 200 mm while it is more than 500 mm in the dry sub-humid region (Table 3) (Benkeblia, 2014). The ground elevation in the south of Sudan can reach 2,200 m, and near the Sudanese-Ethiopian boundaries the elevation can reach 2,700 m (Shahin, 2007).

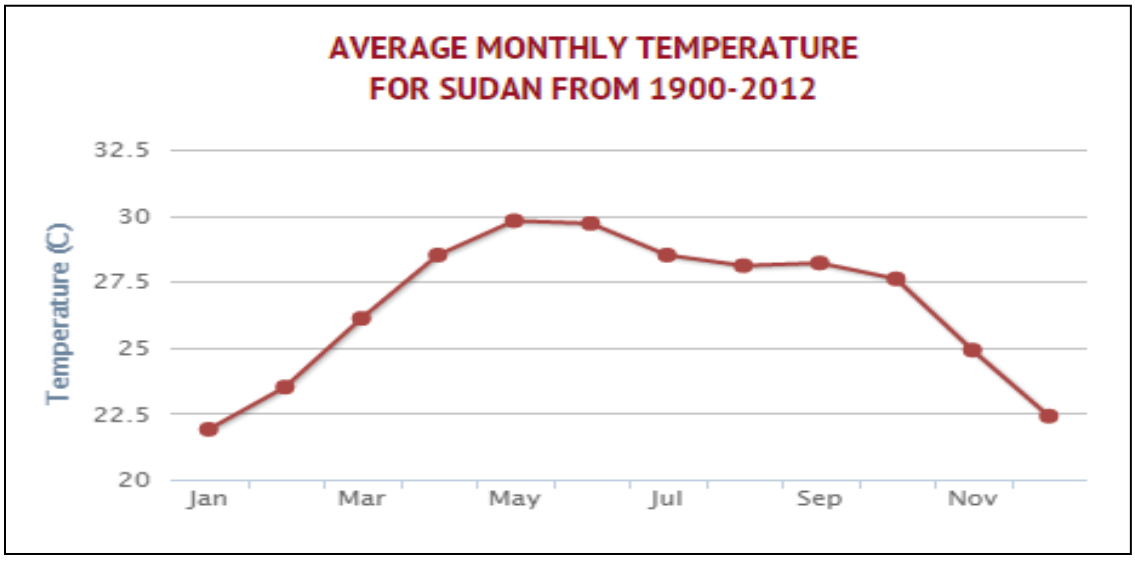

Figure 2: The average monthly temperature for Sudan from 1900 to 2012 (http://sdwebx.world-bank.org/).

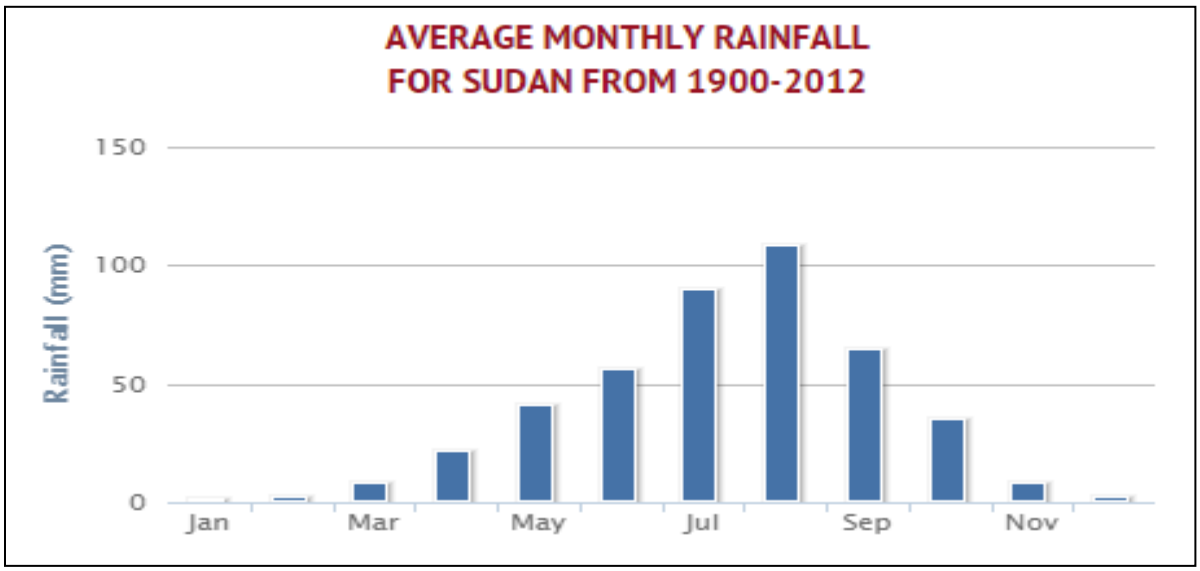

Figure 3: The average rainfall of Sudan from 1900 to 2012 (http://sdwebx.worldbank.org/).

Table 3: *Precipitations in dryland categories (Benkeblia, 2014).*

Classification	Rainfall (mm)	Area (%)
Hyperarid	<200	7.50
Arid	<200 winter or <400 summer	12.1
Semiarid	200- 500 (winter) or 400- 600 (summer)	17.7
Dry subhumid	500- 700 (winter) or 600- 800 (Summer)	9.90
Total		47.2

This study aims to quantify the expansion of the desert areas in Sudan by monitoring and comparing vegetation growth using NDVI, EVI, and GPP from MODIS images through the growing seasonal months: July, August, and September for each of the years 2000, 2009, and 2014. The major factors that lead to the expansion of the desert area will be hypothesized and

analyzed, and the impacts of desertification on the environment and vegetation conditions in the past and present will be discussed.

3.2 Datasets

3.2.1 Remotely Sensed Data

MODIS products were used in this study, including MOD13Q1 and MOD17A (Figure 4). NASA launched the MODIS satellites on board of Terra (EOS AM) and Aqua (EOS PM). Terra covers the earth surface in the morning from north to south while Aqua covers from south to north in the afternoon. Both Terra and Aqua view the earth's entire surface every 1 to 2 days, obtaining data in 36 spectral bands. MODIS satellites are used only for scientific purposes.

MODIS13Q1 and MOD17A2 were obtained from the USGS Science for Changing World (Earth Explorer) (http://earthexplorer.usgs.gov/). The methodology started with downloading two images of MOD13Q1 product for July, August, and September for the years of 2000, 2009, and 2014 with a total of 18 images being acquired. A total of twenty-seven images were collected from MOD17A2 for the growing season months for the years 2000, 2009, and 2014.

MOD13Q1 consists of three bands; band 1 (blue), band 2 (red), and band 3 (near-infrared). The MODIS-derived NDVI and EVI are designed to monitor vegetation conditions. The products are updated every 16 days and are atmospherically corrected for clouds, heavy aerosols, and cloud shadows. GPP product (MOD17A2) is updated every eight days and provides a spatial resolution of 1-km in the Sinusoidal projection. This product is used to compute global energy, carbon, water cycle processes, and vegetation biogeochemistry.

Landsat 8 OLI and Thermal Infrared Sensor (TIRS) data were acquired from the Earth Explorer website (http://earthexplorer.usgs.gov/) for the year 2014 (Table 4; Figure 5). These

images were downloaded based on the accessibility of the data and the percentage of cloud cover. Landsat 8 has 11 bands, bands 1-7 and band 9 with a spatial resolution of 30m, band 8 with a spatial resolution of 15m, and band 10 and band 11 with a spatial resolution of 100m.

Table 4: *The obtained Landsat data for land cover classification.*

Year	Sensor	Path/Row	Acquisition data	Path/Row	Acquisition data	Path/Row	Acquisition data	Path/Row	Acquisition data	Path/Row	Acquisition data	Path/Row	Acquisition data
2014	Landsat 8 OLI/TIRS	179/48	01/15	178/48	11/24	177/48	12/19	176/48	12/28	175/48	12/21		
		179/49	12/09	178/49	09/21	177/49	11/01	176/49	11/26	175/49	11/03		
		180/50	10/05	179/50	10/30	178/50	12/26	177/50	11/01	176/50	09/23	175/50	10/18
		180/51	10/05	179/51	10/30	178/51	11/08	177/51	11/01	176/51	11/26	175/51	11/19
		179/52	12/01	178/52	11/08	177/52	11/01	176/52	11/10	175/52	12/05	174/52	11/28

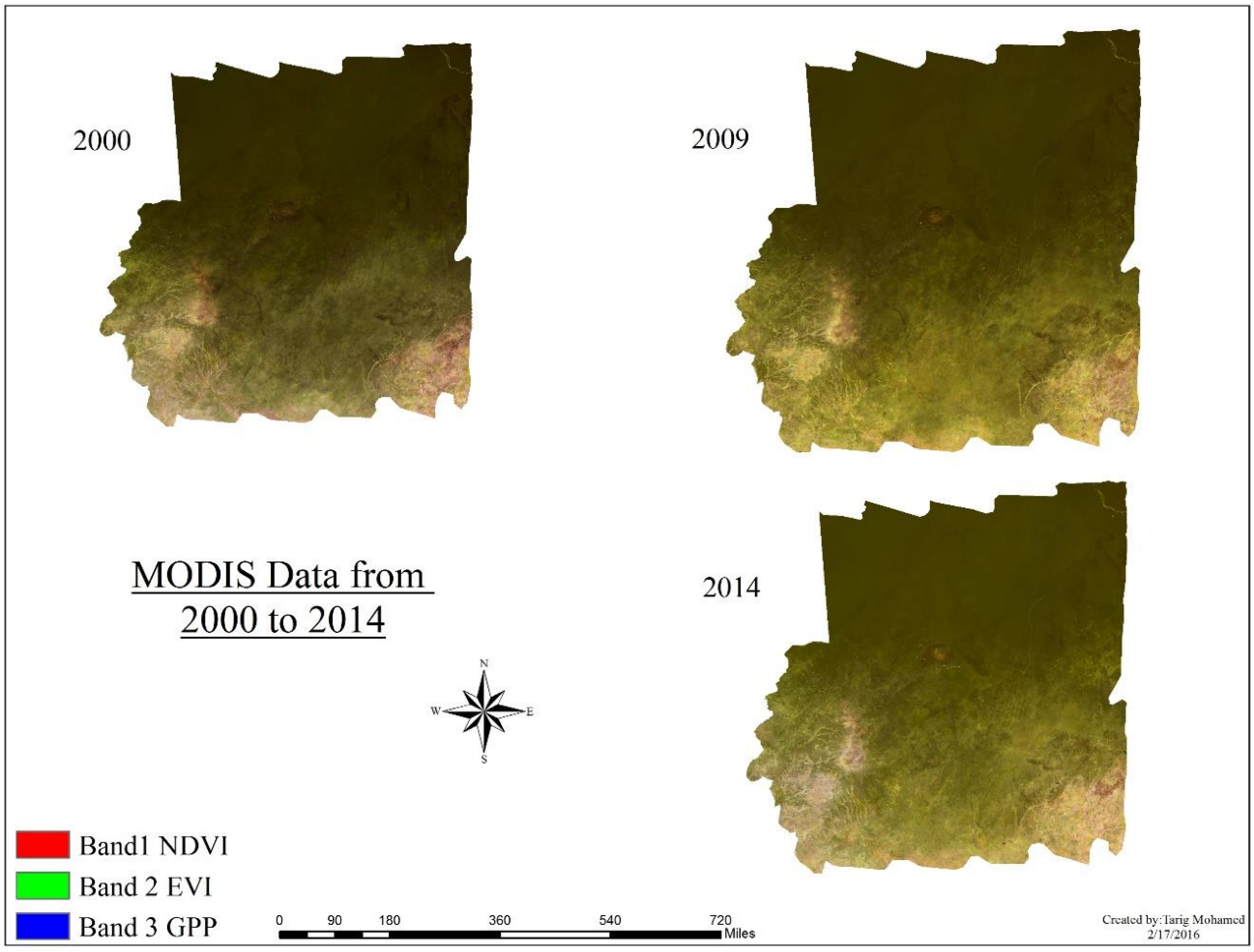

Figure 4: MODIS data before classification.

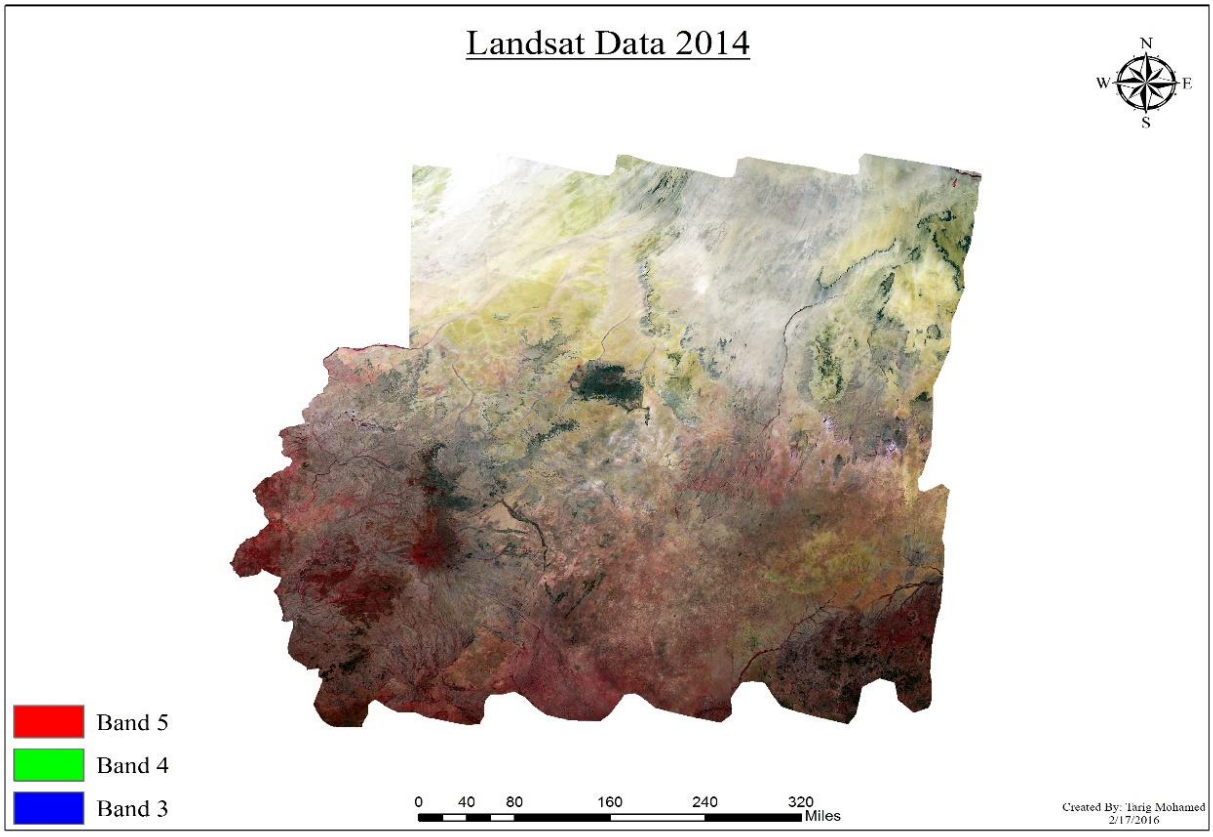

Figure 5: Landsat 8 data before classification.

3.2.2 Population, Precipitation, and Temperature Datasets

Table 5 shows the major factors such as the changes in temperature, precipitation, and population that were investigated to identify the causes and impacts of desert expansion. Temperature and precipitation datasets were downloaded from the National Oceanic and Atmospheric Administration (NOAA) website (http://www.ncdc.noaa. gov/cdo-web/) for the years 1990 to 2013 and presented in Celsius and millimeters respectively. Additionally, population datasets was acquired from the World Bank website (http://data.worldbank.org-/country/sudan) from 1990 to 2014 and presented in millions of people.

Table 5: *The acquired dataset for temperature, precipitation, and population.*

Year	Temperature/ ºC	Precipitation/ mm	Population/ millions
1990	27.7	310.1	20,008,804
1991	27.4	453.2	20,861,117
1992	26.7	399.4	21,820,588
1993	27.4	410.7	22,829,227
1994	27.1	450.2	23,805,536
1995	27.5	427.1	24,691,970
1996	27.7	411.9	25,466,387
1997	27.9	414.6	26,149,124
1998	27.8	437.7	26,777,059
1999	27.5	493.9	27,406,808
2000	27.6	427.4	28,079,664
2001	27.8	406	28,805,142
2002	28.1	393.1	29,569,978
2003	28.2	466.4	30,365,586
2004	28.3	367.7	31,176,209
2005	28.5	407.8	31,990,003
2006	28.2	455.6	32,809,056
2007	28.3	498.6	33,637,960
2008	28.5	442	34,470,138
2009	28.8	346.3	35,297,298
2010	29.2	464.1	36,114,885
2011	28	401.5	36,918,193
2012	28.2	430.5	37,712,420
2013	28.3	444.2	38,515,095
2014	-	-	39,350,274

3.3 Methodology

Figure 6 illustrates the methods used in this study. The first step was to acquire the datasets (MODIS and Landsat images) used in this study. Second, LULC classification was conducted for each of the MODIS and Landsat images using ANN and SMA methods for the years 2000, 2009, and 2014. Third, accuracy assessment for the classified images was carried out. Then desertification expansion was derived using a post-classification change detection method. Furthermore, the results of the MODIS and Landsat images were compared. The major factors and the impacts on environment and vegetation condition in the past and present were explored.

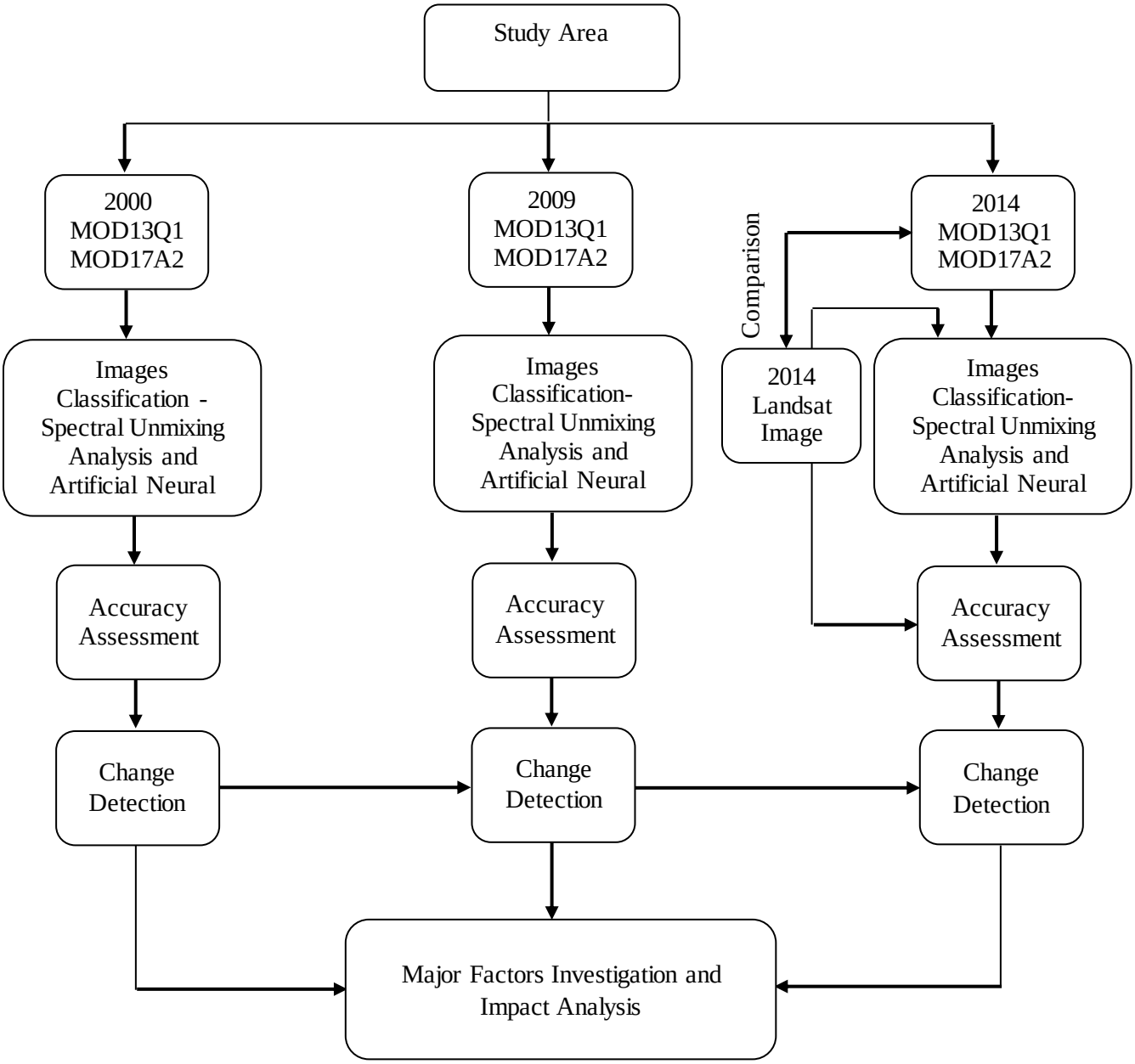

Figure 6: Framework of Methodology.

3.3.1 Image Preprocessing

Image preprocessing is an important procedure in the remote sensing analytical workflow and it involves rehabilitation, restoration, and rectification of the images. The MODIS Re-projection Tool (MRT) was utilized to process the acquired MODIS data. The output projection was adjusted to the Universal Transverse Mercator (UTM) projected coordinate system, zone 35N with datum WGS 1984. The output file format was set as (TIF), so that data can be directly uploaded in ArcMap and ERDAS Imagine. The data processing included calculating the average of NDVI, EVI, and GPP images using Model Maker in ERDAS Imagine.

The Landsat 8 images were radiometrically corrected using ATCOR in ERDAS IMAGINE. This process was used to correct the impact of the remote sensor, sun angle, atmospheric scattering, and absorption. A total of 28 Landsat 8 images were mosaicked to cover the study area, and a color balance technique was used to remove the variation in the scene. A Google Earth image was downloaded and geometrically rectified to WGS_1984_UTM_zone 35N using GCPs. A second order polynomial was used to obtain RMSE of less than one pixel.

3.3.2 Classification

The image classification using the remotely sensing data was carried out using SMA in ENVI software and ANN in TerrSet software. The MODIS data were grouped into four land cover classes: vegetation area, desert, rock, and mountains. The vegetation class consisted of forest, grassland, and other vegetation growing in the arid and semi-arid area (Table2). The water class consisted of lakes and the Nile River. From the Landsat data, five categories were identified vegetation, desert, rock, water, and limestone. To address the mixed pixel problem,

SMA and ANN were used and compared to determine which method would produce the optimal classification results.

3.3.2.1 Spectral Mixture Analysis (SMA)

SMA is a promising method developed from the efforts of earth and planetary scientists (Manal, 2007). In this study, three endmembers (that is, objects consisting of pure pixels) were defined from the MODIS data including sand, water, and vegetation. However, four endmembers were selected from the Landsat data including desert, vegetation, water, and rock. To obtain the endmember fractions for each pixel, SMA was applied to both the MODIS and Landsat data. SMA is an advanced technique for image information extraction, which deduces the fractions (abundances) of the endmembers. In SMA method, the reflectance of a pixel (p'_λ) is determined by the sum of the reflectance values of the endmembers multiplied by their fractions:

$$\rho'_\lambda = \sum_{i=1}^{n} f_i \rho'_{i\lambda} + \varepsilon_\lambda \quad (1)$$

Where ($\rho'_{i\lambda}$) is reflectance value of endmember i for a band (λ), f_i is the fraction of the endmember, N is the number of the endmembers, and ε_λ is the residual error. The fractions of the endmembers are commonly constrained by:

$$\sum_{i=1}^{N} f_i = 1 \quad (2)$$

Model fitting is assessed using the model residuals ε_λ or the RMSE:

$$\text{RMSE} = \sqrt{\frac{\sum_{i=1}^{m} \varepsilon_\lambda^2}{m}} \quad (3)$$

Where M is the number of the bands. The procedure of SMA involves: 1) determining the inherent dimensionality of the data using the Minimum Noise Fraction (MNF) transform; 2)

deriving the Pixel Purity Index (PPI); 3) applying the model to the entire image to obtain the sand, vegetation, and water fraction of all pixels.

3.3.2.2 Artificial Neural Network (ANN)

ANN is a kind of artificial intelligence methods that is capable of improving the classification accuracy based on previous studies. ANN is based on biological neural networks that consist of an affiliated group of neurons, and each neuron contains a single computation process (Zhou and Yang, 2008). ANN can be divided into feedforward network and feedback network. To understand and implement the multi-layer perceptron (MLP), feedforward back-propagation was used in this study.

MLP consist of interconnected neurons or nodes that are representing a nonlinear relationship between an input vector and an output vector (Gardner and Dorling, 1998). The nodes are connected by weights and output signals that are a function of the sum of the inputs to the node modified by a nonlinear transfer function. The fundamental concept of traditional backpropagation learning algorithm is the repeated application of the chain rule to compute the partial derivative, $\partial E/\partial \omega_{ij}$ and once the derivative is known, a gradient descent for minimizing error function is performed

$$\omega_{ij}^{(t+1)} = \omega_{ij}^{(t)} - \eta \frac{\partial E}{\partial \omega_{ij}}^{(t)} \quad (4)$$

Where t is the step of iteration, and η is the learning rate.

3.3.3 Change Detection

After the image classification process, a post-classification change detection method was used to quantify the changes that had occurred in the study area. The entire process was carried out using the Land Change Modeler software function in TerrSet IDRISI software. The software calculates the expansion and contraction of LULC by comparing the classified map of 2000 with the classified map of 2009, the classified map of 2009 with the classified map of 2014, and the classified map of 2000 with the classified map of 2014.

3.3.4 Accuracy Assessment

Accuracy assessment is performed to quantify the agreement between the classified image and the reference image. A Google Earth image was downloaded to be used as a reference image for the Landsat data. The 2014 Landsat data were used as a reference image to carry out and validate the accuracy of the 2000, 2009, and 2014 MODIS data. The accuracy assessment of the year of 2000 and 2009 MODIS data contained uncertainty. Visual interpretation was used to detect whether each pixel is considered as a desert or not. Accuracy assessment was carried on the classified maps of MODIS and Landsat data with a total of 210 and 170 pixels randomly selected respectively. The final accuracy report was generated based on the random sample points on the reference and classified maps. The entire process of accuracy assessment was established in ERDAS IMAGINE 2014.

CHAPTER 4

RESULTS

This chapter consists of four parts: 1) the results of two classification methods (SMA and ANN) for three years, 2) the results of the accuracy assessment, 3) the result of the land cover change for two periods of three years, and 4) the major factors of the desert expansion.

4.1 Image Classification and Accuracy Assessment

The results of the classified images depicted the changes in land cover categories within the study area and gave the quantitative view of the desert expansion. The accuracy assessment demonstrated a desirable overall classification for the land cover categories.

4.1.1 Landsat Data Using Artificial Neural Network ANN

Figure 7 shows a classification map of Landsat data for the year of 2014 using ANN. Five land cover categories were identified, including vegetation, water, desert, rock, and limestone. This map identified the recent extent of the desert area. From the map, vegetation is located in the southern and northern parts of the study area. Rock is located in the northern and northeastern parts of the study area. Due to misclassification, some pixels were classified as vegetation while it was actually rock. Water has a small area, and is located in the northern and southern regions of the study area. Limestone occurs in the eastern, northern, and northwestern parts of the study area.

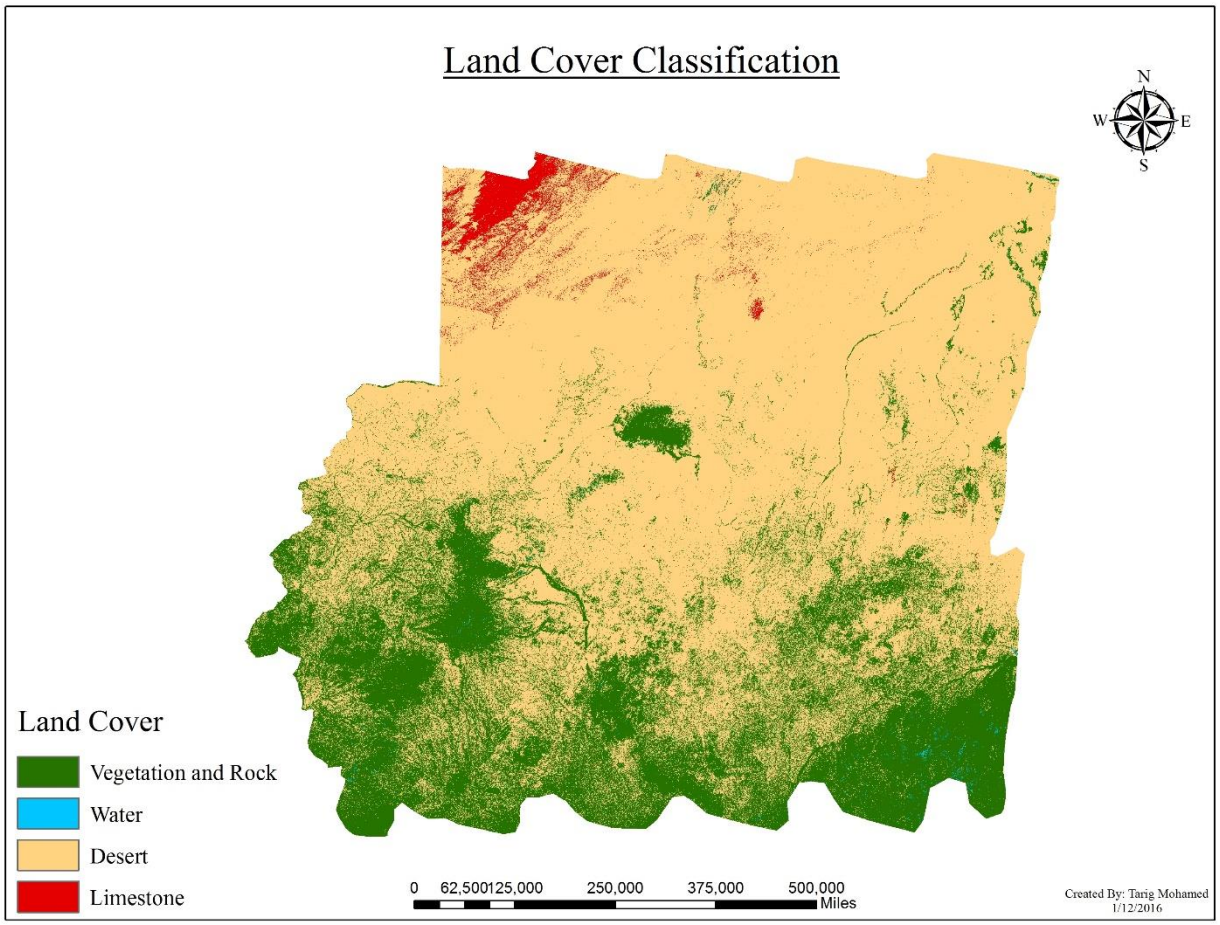

Figure 7: A map showing the land cover classification of Landsat data 2014 using ANN.

Compared with the Google Earth image, the land cover classification of Landsat data for 2014 was visually interpreted and assessed. The overall classification accuracy and kappa statistics was 86.47 % and 78.37 % respectively (Table 6). These percentages confirm the agreement between the classified image and the reference image. The producer accuracy was 89.74 %, 100 %, 79.71 %, and 95.24 % of vegetation, water, desert, and limestone respectively. The corresponding user accuracy was 87.50 %, 20 %, 91.67 %, and 100 % for the same classes respectively. Water had the highest omission error with 80 % of its pixels being assigned to other classes. Vegetation and desert had an omission error of 12.5 % and 8.3 % respectively.

Limestone had no omission error. Desert had the greatest commission error of 20.3 % for the pixels sloped to an incorrect class. Vegetation and limestone had commission errors of 10.3 % and 4.8 % respectively; Water had no commission error.

Table 6: *Error matrix of 2014 Landsat data and ANN classification.*

Classified Data	2014	Reference Data						
		Vegetation	Water	Desert	Limestone	Xi+	User A%	C.K
	Vegetation	**70**	0	10	0	80	87.50 %	0.7690
	Water	4	**2**	4	0	10	20 %	0.1905
	Desert	4	0	**55**	1	60	91.67 %	0.8597
	Limestone	0	0	**0**	**20**	20	100 %	1.0000
	X+J	78	2	69	21	170		
	Prod A %	89.74 %	100 %	79.71 %	95.24 %			
	Overall classification accuracy = 86.47%, Overall kappa statistics = 0.7837							

4.1.2 Landsat Data Using Spectral Mixture Analysis (SMA)

Figure 8 indicates the classification maps of Landsat data for the year of 2014 using SMA classification. SMA produced four fraction maps vegetation fraction, desert fraction, rock fraction, and water fraction. From the fraction vegetation map, we can see that vegetation is concentrated in the eastern, southern, southwestern, and central parts of the study area. However, the desert covered a large area in the north and a small area in the south. Water occupies a small parts in the east and south area of the study area. Due to the turbid some desert and rock areas were incorrectly classified into water. From the rock fraction map, rocks are predominantly located in the north, west, south, and northeast parts of the study area.

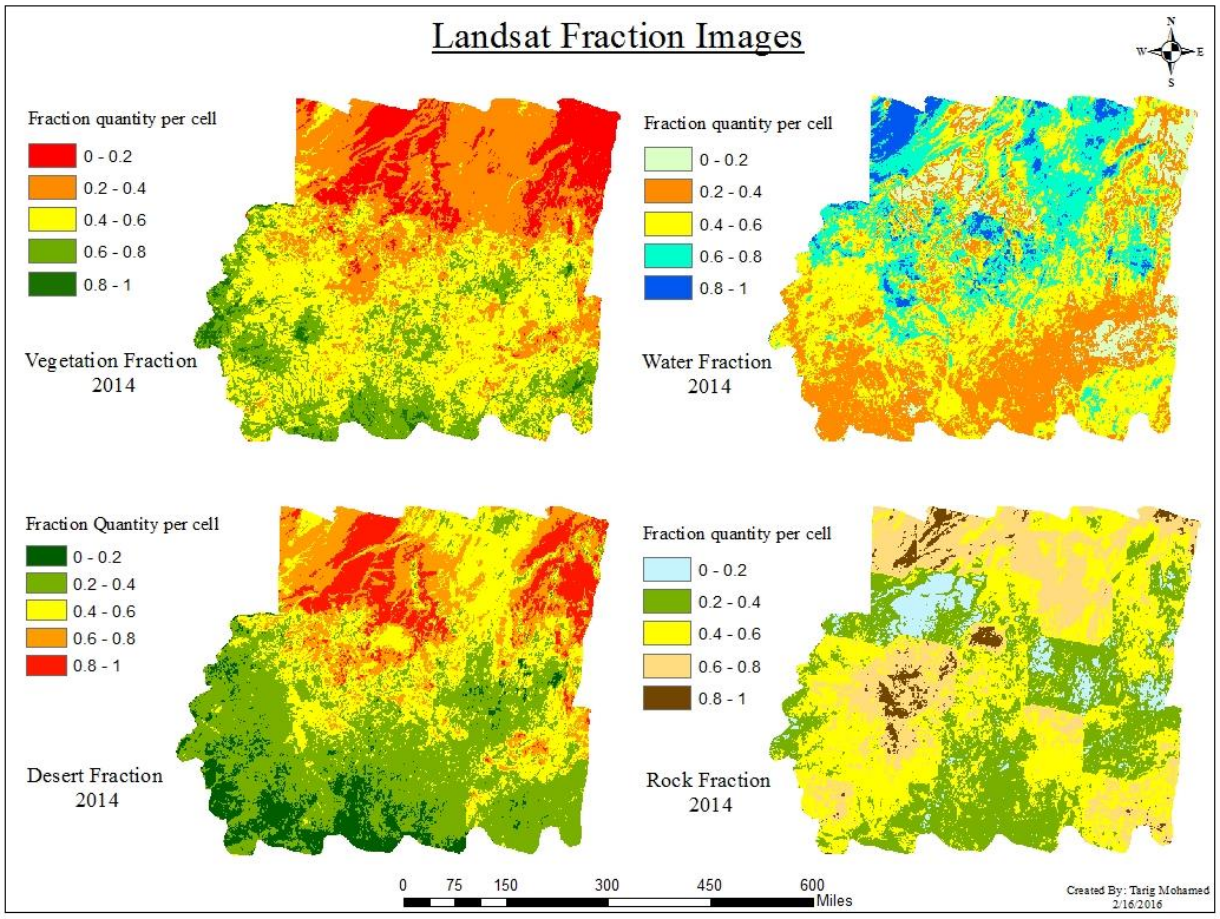

Figure 8: Maps showing the fraction quantity per cell of Landsat 2014 data.

4.1.3 MODIS Data Using ANN

Figure 9 indicates the MODIS image derived land cover classification maps for three years 2000, 2009, and 2014 using ANN. From these maps, it was noticed that vegetation was located on the south side, desert situated in the north and south side. Rock occurs in the north, northeast, and central parts of the study area. We can visually recognize the change in the land cover between 2000 and 2014. During the past 14 years, desert expansion increased gradually in the south portion of the study area. Additionally, from 2000 to 2014, vegetated area receded in the northeastern portion of the study area. Compared to 2000, for both years 2009 and 2014,

vegetated lands transitioned into desert in the southern portion of the study area. In ANN, mountains and rocks were combined, and demonstrated negligible change.

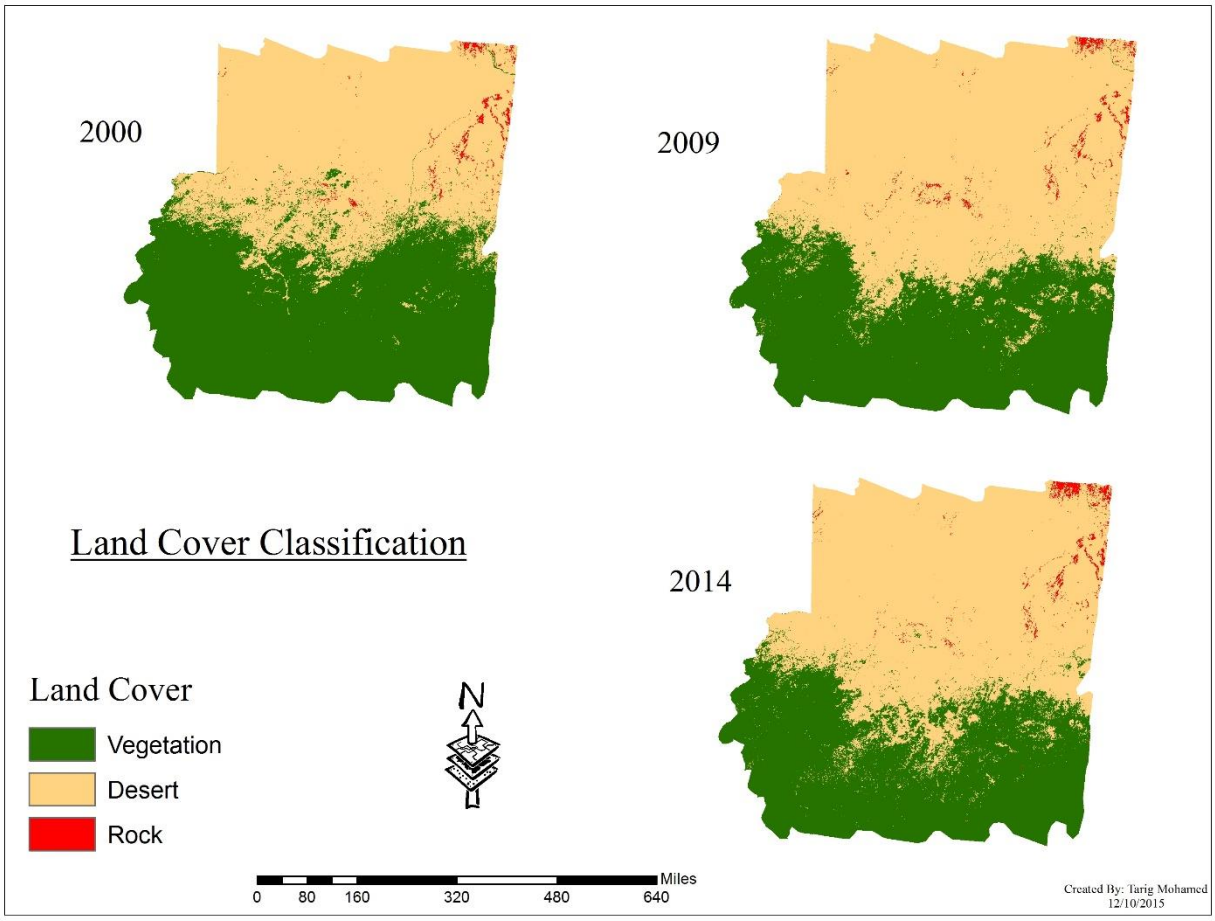

Figure 9: Land cover classification using ANN and MODIS images for years 2000, 2009, and 2014.

The classification performance of land cover types of 2000, 2009, and 2014 were achieved. Error matrices were produced for each of the maps by comparing them with the reference map. A total of 100 random points for vegetation, 80 random points for desert, and 30 random points for rock and mountains were generated and used for the accuracy assessment.

Overall accuracy, user's and producer's accuracies, kappa coefficient, and the overall kappa value were calculated from the error matrix.

The overall classification accuracy and kappa statistics of 2000 map was 79.52% and 66.47 % respectively (Table 7). This was the lowest classification accuracy percentage compared to those of other years, and it demonstrated an acceptable agreement between the classified image and the reference image. The producer accuracy (omission error) was 87.91%, 74.44%, and 68.97% for vegetation, desert, and rock respectively. On the other hand, the user accuracy (commission error) was 80%, 83.75%, and 66.67% respectively, for the corresponding classes.

Rock showed the highest omission error of 33.3% of its pixels being assigned to other categories. Vegetation had an omission error of 20%, and its pixels were assigned to desert or rock. Desert had the lowest omission error of 16.25 %, and its pixels were assigned to vegetation or rock. Vegetation, desert, and rock had a commission error of 12.1%, 25.6%, and 31.03% respectively. Thus, each category had pixels that were incorrectly classified into a particular class while it belonged to another class.

Table 7: *Error matrix of 2000 ANN and MODIS image classification.*

Classified Data	2000	Reference Data					
		Vegetation	Desert	Rock	Xi+	User A%	C.K
	Vegetation	**80**	15	5	100	80%	0.6471
	Desert	9	**67**	4	80	83.75%	0.7156
	Rock	2	8	**20**	30	66.67%	0.6133
	X+J	91	90	29	210		
	Prod A %	87.91%	74.44%	68.97%			
	Overall classification accuracy = 79.52%, Overall kappa statistics = 0.6647						

The overall classification accuracy and kappa statistics for the 2009 map was 81.90 % and 70.36 % respectively (Table 8). The producer accuracy (omission error) was 87.23 %, 76.47

%, and 83.33 % for vegetation, desert, and rock respectively. The corresponding user accuracy (commission error) was 82% for vegetation, 81.25 % for desert, and 83.33 % for rock. Both desert and vegetation had the greatest omission error of 18.75 % and 18 % respectively. Moreover, rock shows the least percentage of omission error of 16.7 % of pixels that were classified into another category. Desert had the highest commission error of 23.5 % of the pixels that is erroneously assigned to an inappropriate class while it is returned to another class. Rock and vegetation had a commission error of 16.7 % and 12.8 % respectively, of the pixels that were assigned into incorrect class.

Table 8: *Error matrix of 2009 ANN and MODIS image classification.*

Classified Data	2009	Reference Data					
		Vegetation	Desert	Rock	Xi+	User A%	C.K
	Vegetation	**82**	16	2	100	82%	0.6741
	Desert	12	**65**	3	80	81.25%	0.6825
	Rock	0	5	**25**	30	83.33%	0.8056
	X+J	94	85	30	210		
	Prod A %	87.23%	76.47%	83.33%			
	Overall classification accuracy = 81.90%, Overall kappa statistics = 0.7036						

The overall classification accuracy and kappa statistics of 2014 map was 84.76 % and 75.27 % respectively (Table 9). This indicated a good agreement between the classified and the reference image. The producer accuracy for vegetation, desert and rock was 93.62 %, 81.48 %, and 68.57 % respectively. The corresponding user accuracy for the same categories was 88 %, 82.50 %, and 80 % respectively. Rock and desert had the greatest percentage of omission error of 20 % and 17.5 % respectively. Vegetation showed the least percentage of omission error of 12 % of its pixels classified into another category. Rock had the highest commission error of 31.43 % of the pixels that was erroneously assigned to an inappropriate class. Desert and vegetation had a

commission error of 18.52 % and 6.4 % respectively, of the pixels that were assigned into inappropriate class.

Table 9: *Error matrix of 2014 ANN and MODIS classification.*

Classified Data	2014	Reference Data					
		Vegetation	Desert	Rock	Xi+	User A%	C.K
	Vegetation	**88**	9	3	100	88%	0.7828
	Desert	6	**66**	8	80	82.50%	0.7151
	Rock	0	6	**24**	30	80%	0.7600
	X+J	94	81	35	210		
	Prod A %	93.62%	81.48%	68.57%			
	Overall classification accuracy = 84.76%, Overall kappa statistics = 0.7527						

4.1.4 MODIS Data Using SMA

Figures 10 to 12 show the classification maps for the years 2000, 2009, and 2014 respectively, after using SMA technique. SMA produced fraction maps for three categories vegetation, desert and water for three years 2000, 2009, and 2014. From the vegetation fraction maps, the green color indicates a high proportion in a given pixel, while the red color indicates a small percentage for that category. From the fraction of desert maps, the red color represent a high proportion in a given pixel, while the green color shows the least percentage of that class. The high vegetation fraction values were located in the south part of the study area. The high desert fraction values were found on the north side. By comparing the magnitude of the desert area in the three maps, we can see that 2000 has the lowest desert area. Also, the direction of the desert expansion is toward to the south and southwest. On the other hand, vegetation showed an enormous change and been replaced by desert particularly in the period of 2000 to 2009. The study area contained a small lake located in the northwest as well as, the Nile River which is located in the north part of the study area. Due to the misclassification the water fraction

produced a similar result as the vegetation and desert fraction. Overall, both SMA and ANN shown the magnitude and direction of the desert expansion from 2000 to 2014.

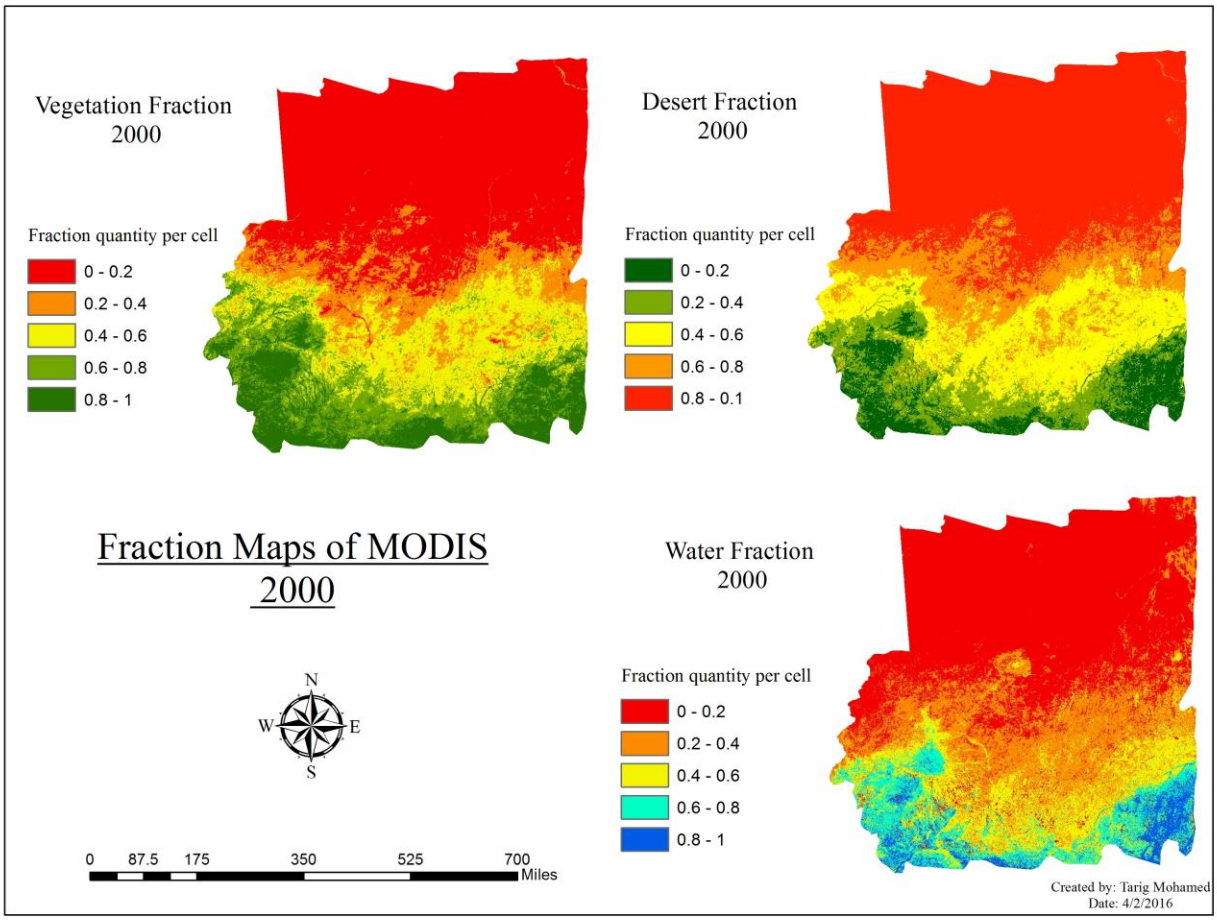

Figure 10: The fraction maps of vegetation, desert and water in 2000.

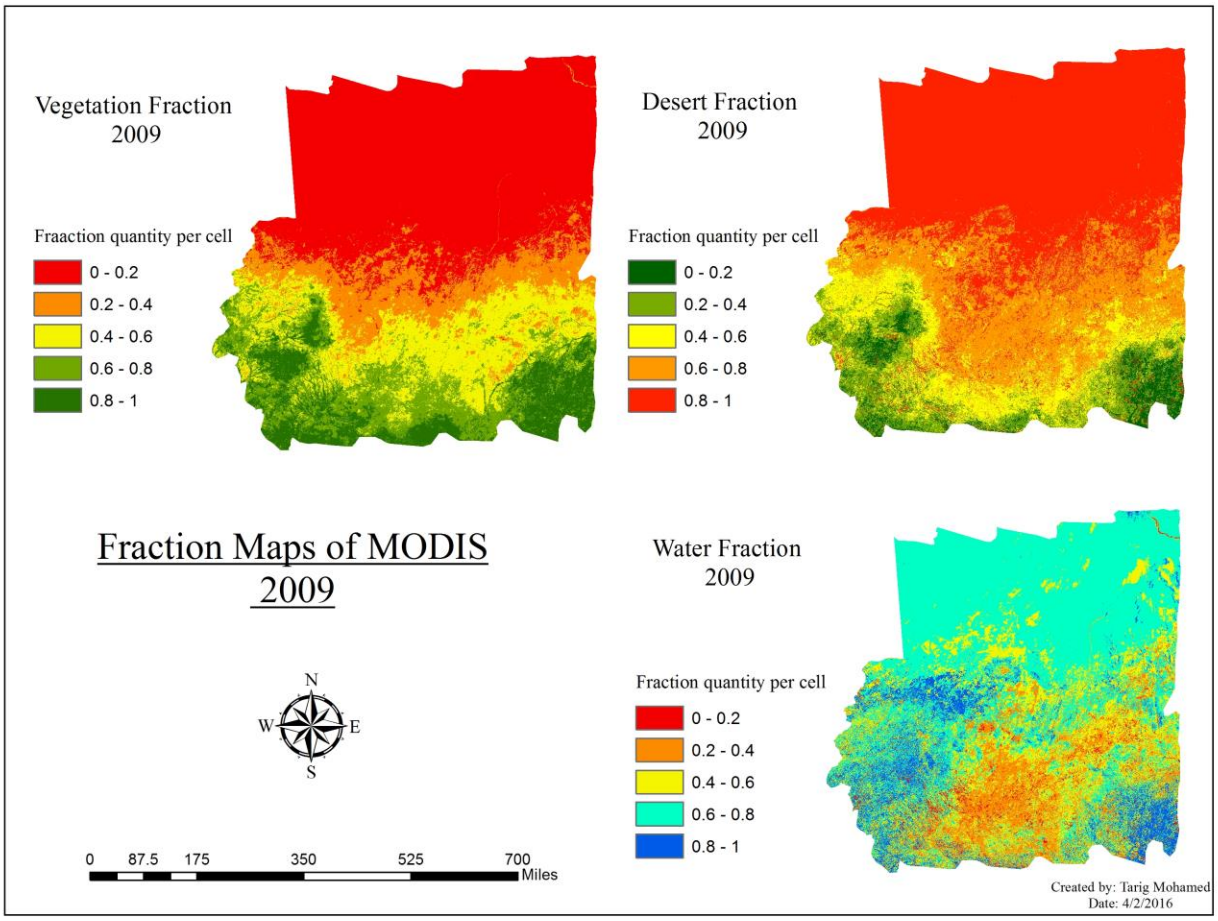

Figure 11: The fraction maps of vegetation, desert and water in 2009.

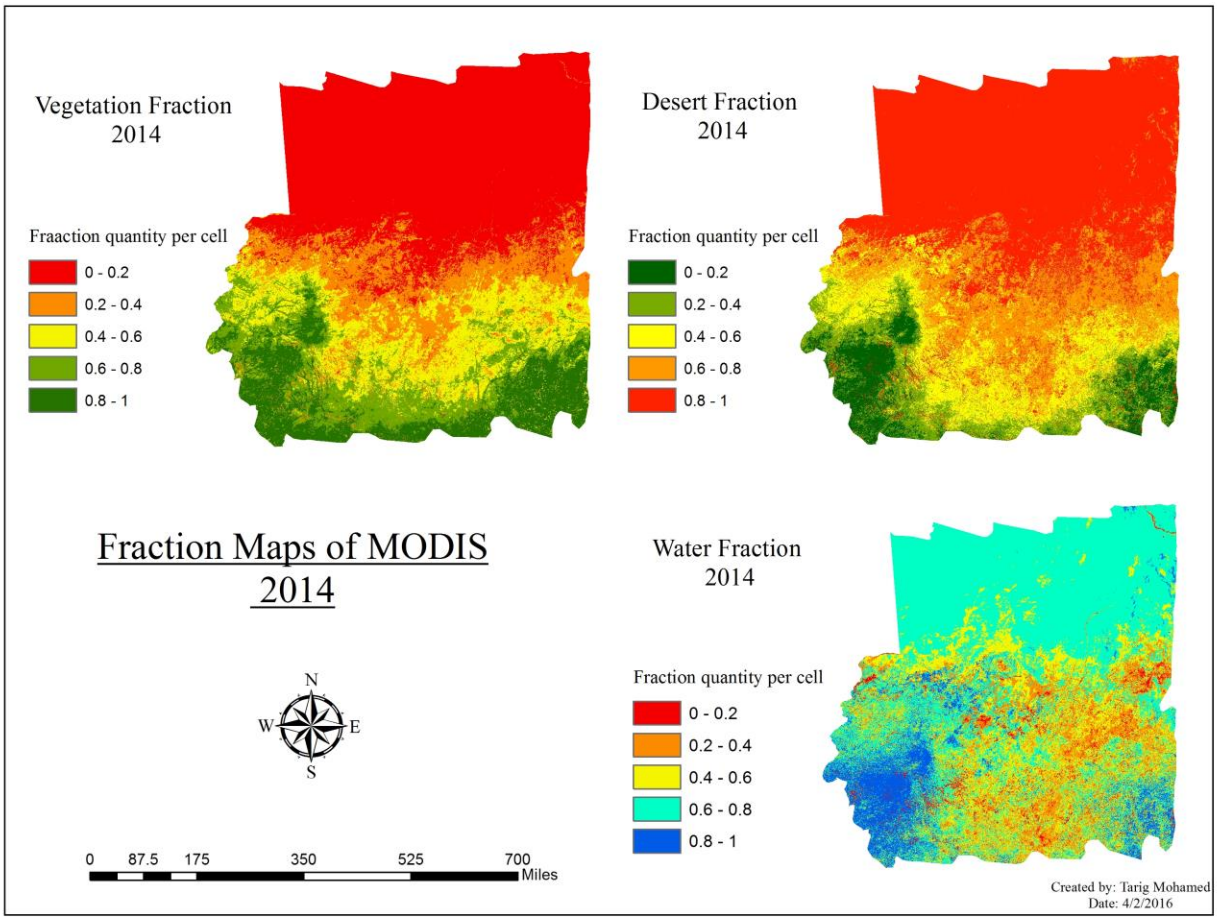

Figure 12: The fraction maps of vegetation, desert and water in 2014.

The classification accuracy assessment for the map of 2014 were carried out. Error matrix were produced by comparing it with the reference map. A total of 140 pixels were acquired from the stratified random sampling design. The overall classification accuracy and kappa statistics of 2014 map was 76.42 % and 58.1 % respectively (Table 10). The producer accuracy was 98.75 %, 38 %, and 90 % for desert, vegetation, and water respectively. The corresponding user accuracy was 86.81 %, 95 %, and 31.03 % respectively, for the same categories. Water demonstrated the highest omission error of 68.97 % of its pixel classified to other classes. Desert and vegetation showed the least percentages of omission error of 13.19 % and 5 % respectively, of its pixels classified into another category. Desert had the lowest percentage of commission error with 1.25

% of the pixels that was incorrectly classified to inappropriate class. Vegetation and water has commission errors of 62 % and10% respectively with the pixels that were classified into incorrect class.

Table 10: *Error matrix of 2014 SMA and MODIS image classification.*

Classified Data	2014	Reference Data					
		Desert	Vegetation	Water	Xi+	User A%	C.K
	Desert	**79**	12	0	91	86.81%	0.964
	Vegetation	0	**19**	1	20	95%	0.277
	Water	1	19	**9**	29	31.03%	0.874
	X+J	80	50	10	140		
	Prod A %	98.75%	38%	90%			
	Overall classification accuracy = 76.42% , Overall kappa statistics = 0.581						

4.2 Land Cover Change

IDRISI Land Change Modeler was used in analyzing the land cover changes for each of the temporal periods. The results of the land cover changes were divided into two sections. The first section shows the results of land cover changes after utilizing ANN and second is the outcome of the land cover changes after applying SMA. Moreover, each section consists of three sub-sections. The first sub- section represents the total gain and loss for each of the land cover categories. The second sub-section represents the net change in each class and is computed by adding the gain and then subtracting the loss. The third sub-section describes the contributors to the net change for each land cover category.

4.2.1 Land Cover Change from ANN Classification

Figure 13 shows the gains and losses in percentage by category for the period 2000 to 2009, 2009 to 2014, and 2000 to 2014. From the figure, we can see that vegetation and desert had the greatest change. Rock appears to have a negligible change throughout the years. By looking at the net change from 2000 to 2009, rock and desert gained a net change of 2.40 % and 12.53 % respectively (Figure 14). However, vegetation acquired a net negative change of 20.87 %. Figure 15 shows that from 2000 to 2009 vegetation lost 6.94% for desert, and rock gained 0.33 % from the desert. From 2009 to 2014 desert acquired a net negative change with a small percentage of 1.49 %. While rock and vegetation gained a net change of 0.29 % and 1.20 % respectively. Vegetation and rock gained 1.21 % and 0.29 % respectively, from the desert. In the whole period of 2000 to 2014, rock and desert gained a net change of 4.36 % and 9.98 % respectively, while vegetation experienced a net negative change of 16.64 %. Vegetation lost 5.73 % for desert and rock gain 0.62 % from the desert (Figure 15).

Figure 13: Gains and losses in percentage for each of categories in the study area.

Figure 14: Net change in percentage for each of categories in the study area.

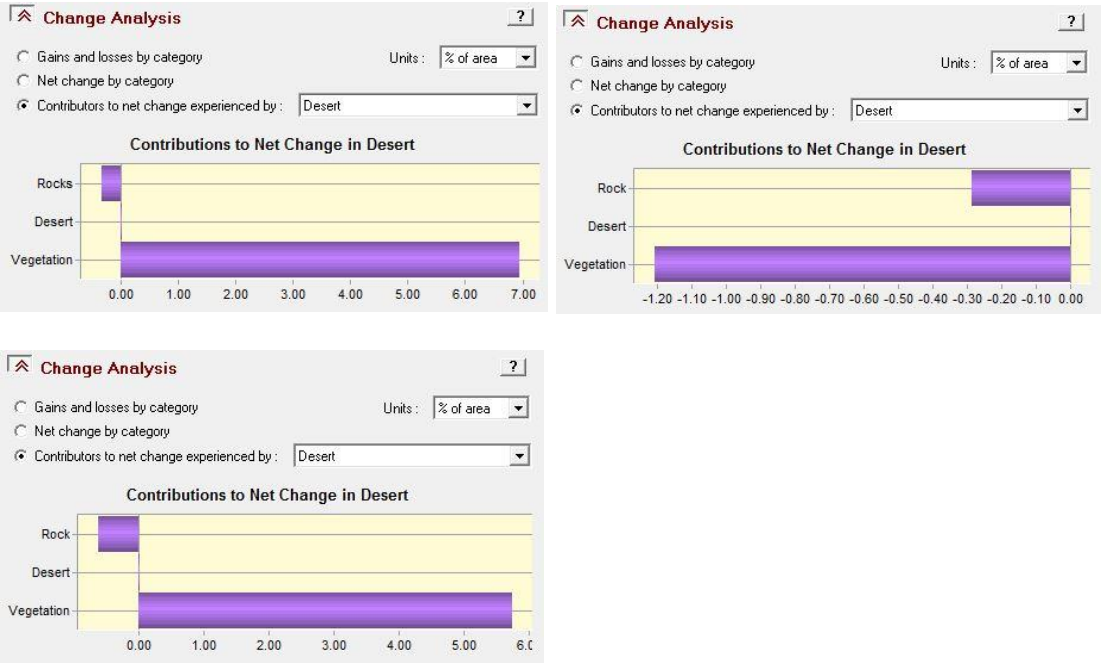

Figure 15: Contributors to net change of the desert areas.

Tables 11 to 13 show cross-tabulation matrices in percentages to access the results of the land cover change from 2000 to 2009, from 2009 to 2014, and from 2000 to 2014. From the tables, the numbers that highlighted in bold indicate the overall percentage of persistence for a particular category between two years. The loss column displays the total percentage that has been lost in an individual category between years and is calculated by subtracting the column total of a certain category from the persistence of the same category. The gain row shows the total percentage that has been acquired and was calculated by subtracting the total of a specific row from the persistence of the same category. Desert had the highest persistence percentage among other classes 45.39 % (Table 11), 49.5 % (Table 12), and 44.74% (Table 13). Figure 16 shows the gain, losses and persistence of the desert area, and it emphasizes that the desert has been expended during 2000 to 2014.

Table 11: *Cross-tabulation matrix in percentage comparing the 2000 classification map and the 2009 classification map.*

	2009					
	Categories	Vegetation	Desert	Rock	Total	Loss
2000	Vegetation	**33.11**	7.09	0	40.21	7.1
	Desert	0.16	**45.39**	0.58	46.12	0.73
	Rock	0	0.24	**13.42**	13.67	0.25
	Total	33.27	52.73	14	100	
	Gain	0.16	7.34	0.58		

Table 12: *Cross-tabulation matrix comparing the 2009 classification map and the 2014 classification map.*

	2014				
	Vegetation	Desert	Rock	Total	Loss
Vegetation	**31.83**	1.43	0	33.27	1.44
Desert	2.64	**49.5**	0.59	52.73	3.23
Rock	0	0.3	**13.7**	14	0.3
Total	34.47	51.24	14.29	100	
Gain	2.64	1.74	0.59		

2009

Table 13: *Cross-tabulation matrix comparing the 2000 classification map and the 2014 classification map.*

	2014				
	Vegetation	Desert	Rock	Total	Loss
Vegetation	**33.99**	6.21	0.01	40.21	6.22
Desert	0.48	**44.74**	0.9	46.12	1.38
Rock	0	0.28	**13.39**	13.67	0.28
Total	34.47	51.24	14.29	100	
Gain	0.48	6.5	0.9		

2000

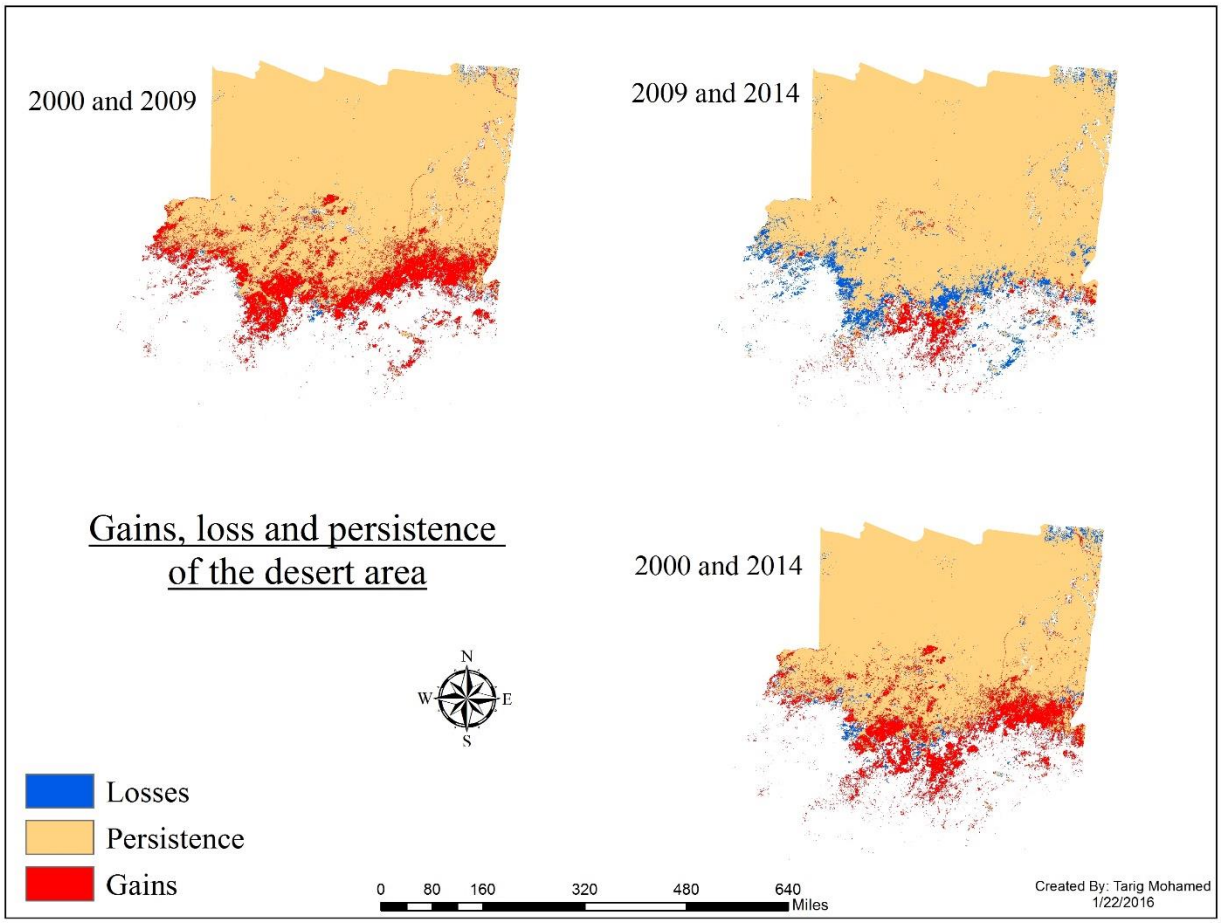

Figure 16: Gains, losses and persistence of the desert area using ANN classification.

4.2.2 Land Cover Change from SMA Classification

Figure 17 indicates the gain and loss in percentage for two categories (desert and vegetation). Desert experienced the greatest change between 2000 and 2009. Figure 18 shows the net change for each category and desert gained a net change of 5.31 %. However, vegetation experienced a net negative change of 17.71 %. Vegetation lost 4.09 % for desert (Figure 19). From 2009 to 2014 desert acquired a net change of 4.25 %. However, vegetation experienced a net negative change of 17.21 %. From 2000 to 2014, desert gained a net change of 9.27 %. However vegetation experienced a net negative change of 37.77 %. The maps of figure 20 show

the gain, losses, and persistence of the desert area, and the maps confirmed that the desert has been expended during the last 14 years.

Figure 17: Gains and losses per hectares in the two categories found in the study area.

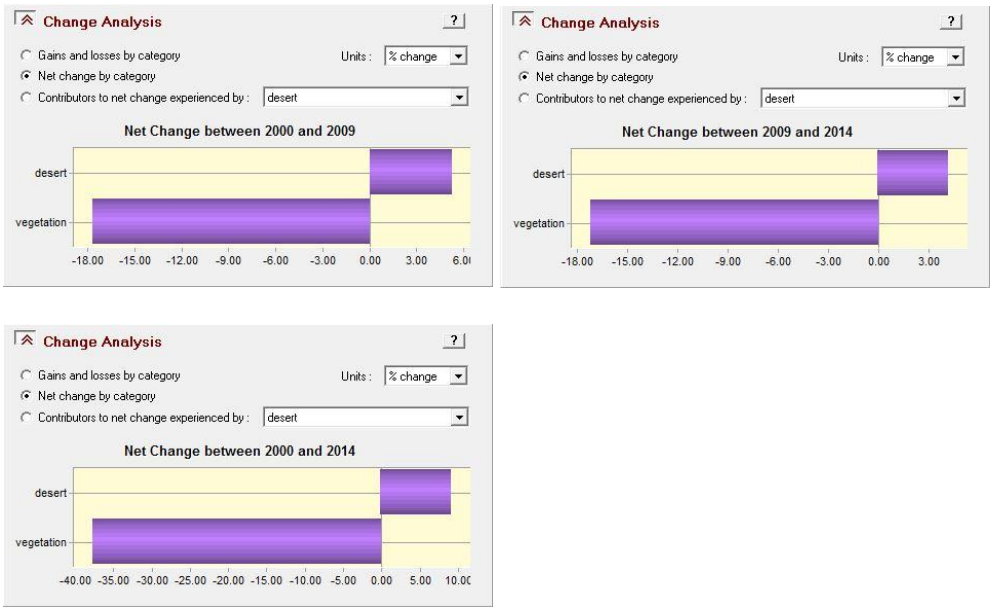

Figure 18: Net change per hectares in the two categories found in the study area.

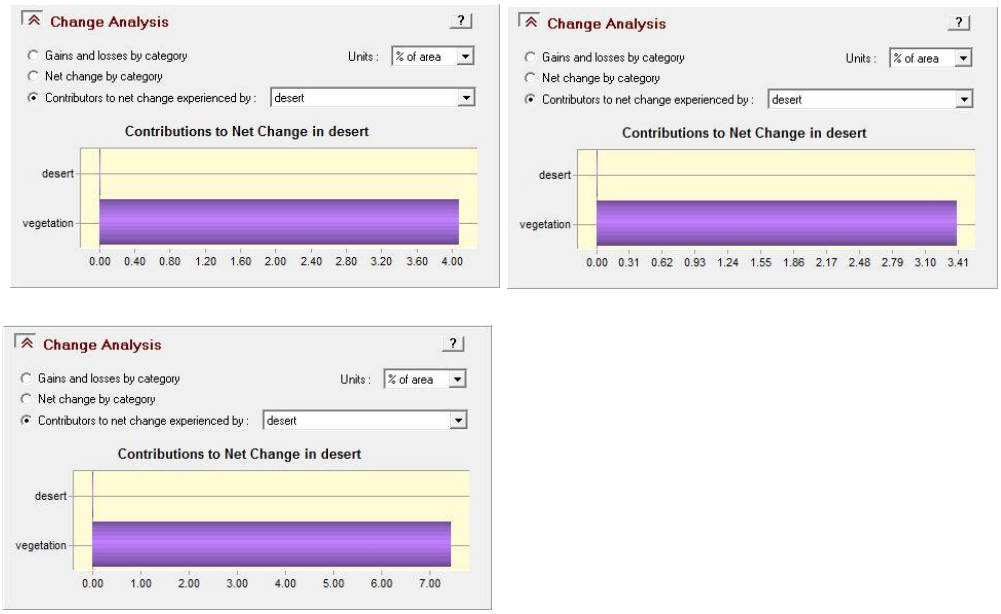

Figure 19: Contributors to net change of the desert areas.

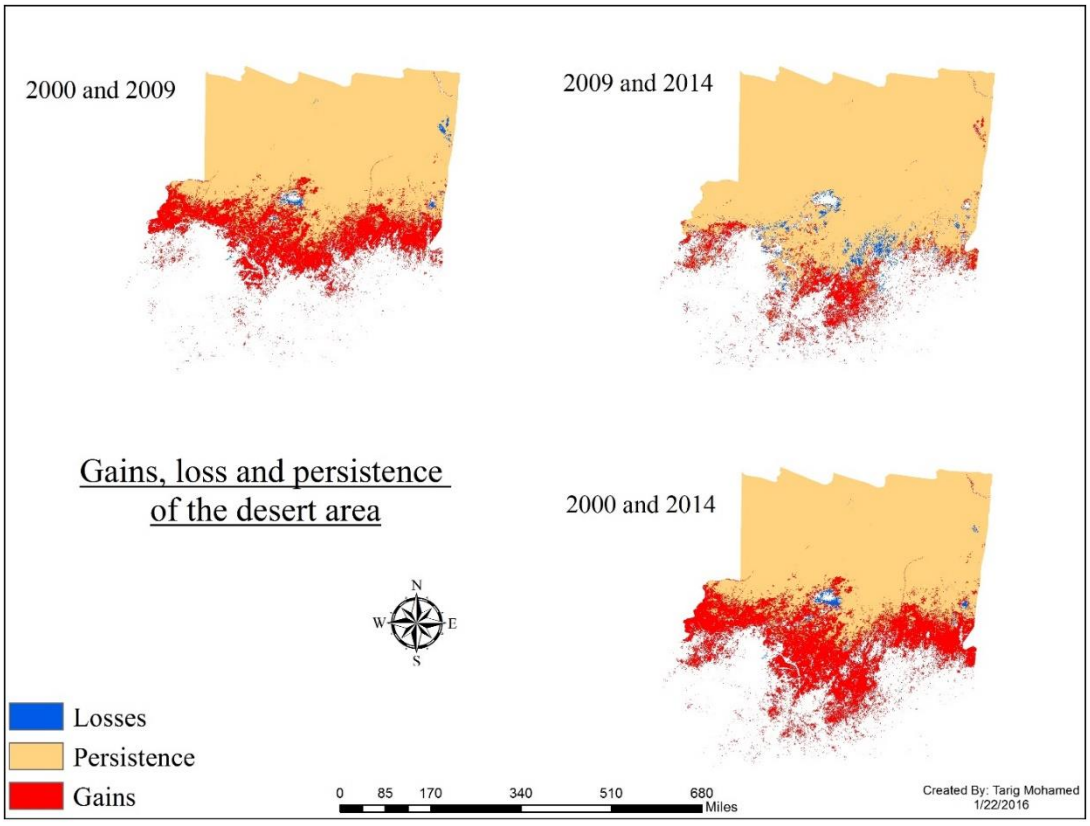

Figure 20: Gains, losses, and persistence of the desert area using SMA classification.

4.3 Major Factors of Desertification

Population growth, temperature change, and precipitation change were hypothesized to have led to the expansion of desert in this study.

4.3.1 Population Increase

The population of the Republic of Sudan has increased gradually from 1990 to 2014 (Figure 21). In 1990, the total population of Sudan was 20 million people. However, it exploded to 39.35 million in 2014. The population increase in Sudan was not confined only to the urban areas such as Khartoum, but also in the rural regions such as Darfur, Kordofan and Alschemaliya states as well (Figure 22). In 2009, the total population of Darfur, Kordofan, and Alschemaliya States was 7.7 million, 4.5 million, and 720 thousand people respectively. However, in 2014 each state has a total population of 8.6 million, 4.9 million, and 835 thousand people. From 2000 to 2009 the population of Sudan rose by 7.09 million. Similarly, the desert area had increased by 12.53 % from 2000 to 2009 (Figur 23). From 2009 to 2014, the population increased by 3.96 million. However, the desert expansion declined by 1.49 %. From 2000 to 2014 the total population increased by 11.15 million people. On the other hand, the desert expansion also increased by 9.98 %.

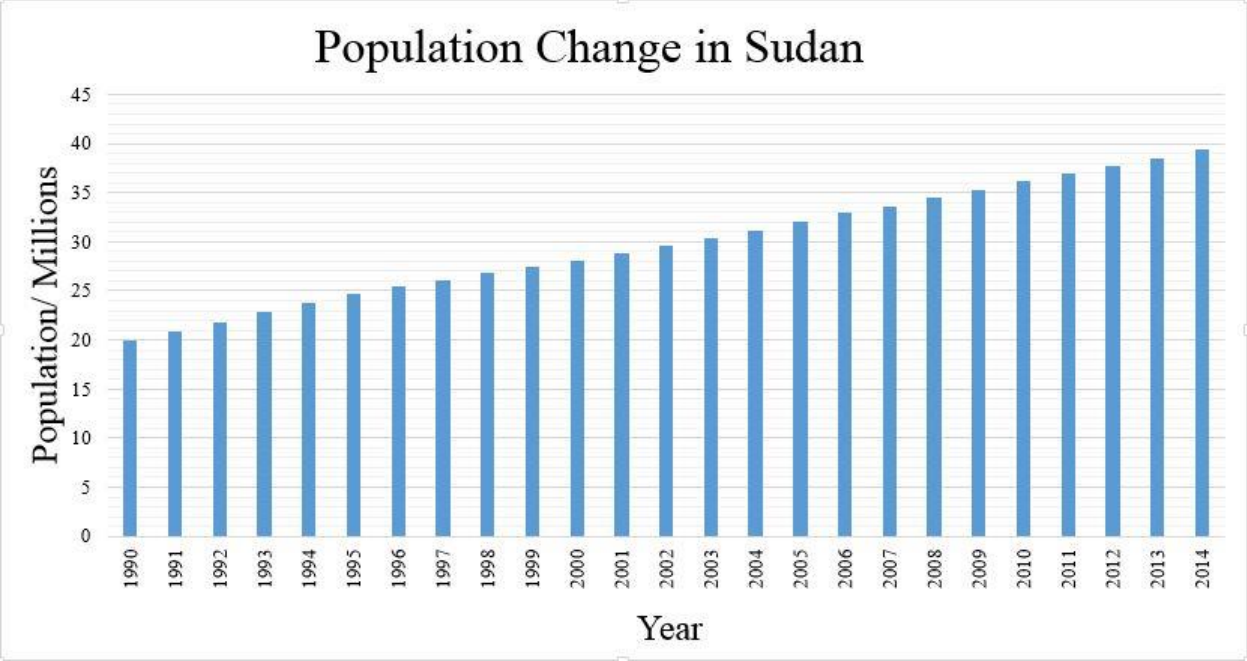

Figure 21: The population change in Sudan from 2000 to 2014 in million.

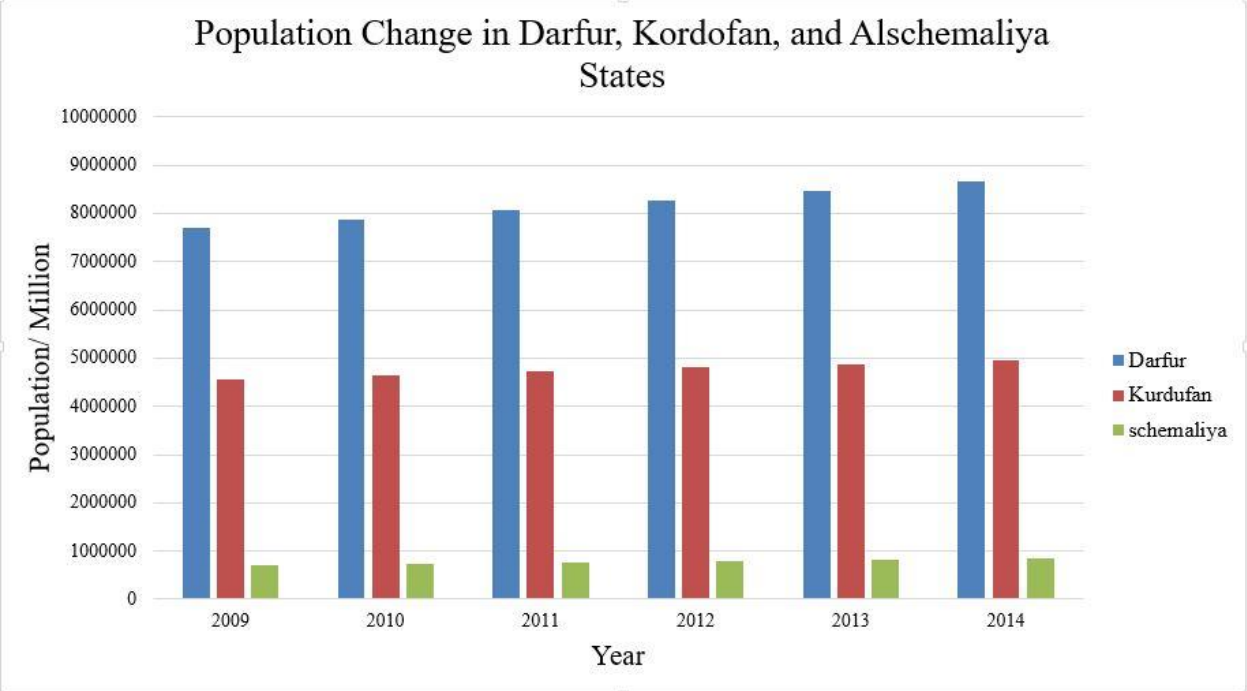

Figure 22: The population change in the driest states in Sudan.

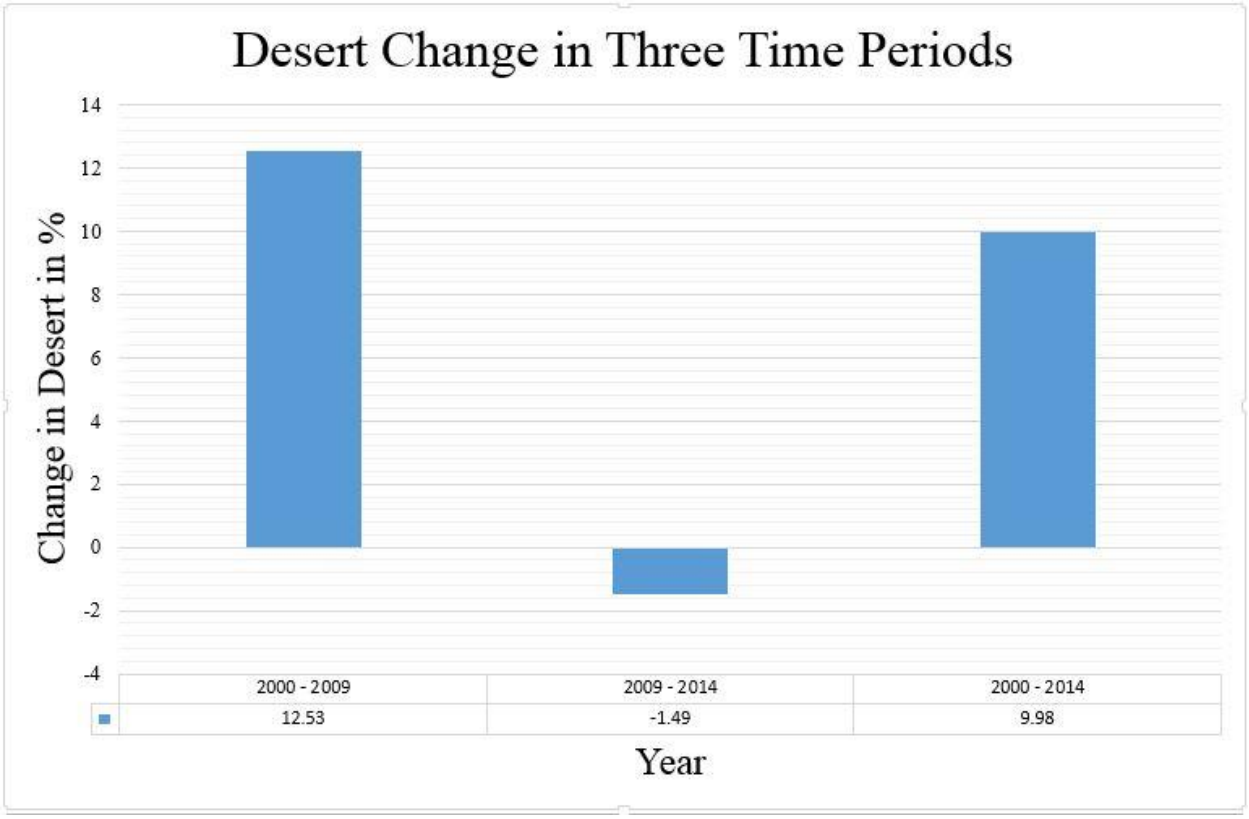

Figure 23: The desert change in three time periods.

4.3.2 Temeperature

Figure 24 displays the average change in temperature from 1990 to 2013. In 1990 the temperature was 27.7 ºC, however, in 2013 it was 28.3 ºC. From the graph, 2010 was the warmest year with an average temperature of 29.2 ºC. However, 1992 was the coldest year with an average temperature of 26.7 ºC. From 2000 to 2009 the temperature increased steadily from 27.6 ºC to 29.2 ºC. During the same period, the expansion of the desert also increased (Figure 23). From 2009 to 2013, the temperature dropped to 28.3 ºC. The corresponding desert expansion also decreased. From 2000 to 2013 the average temperature rose by 0.6 ºC. The desert

expansion also increased.

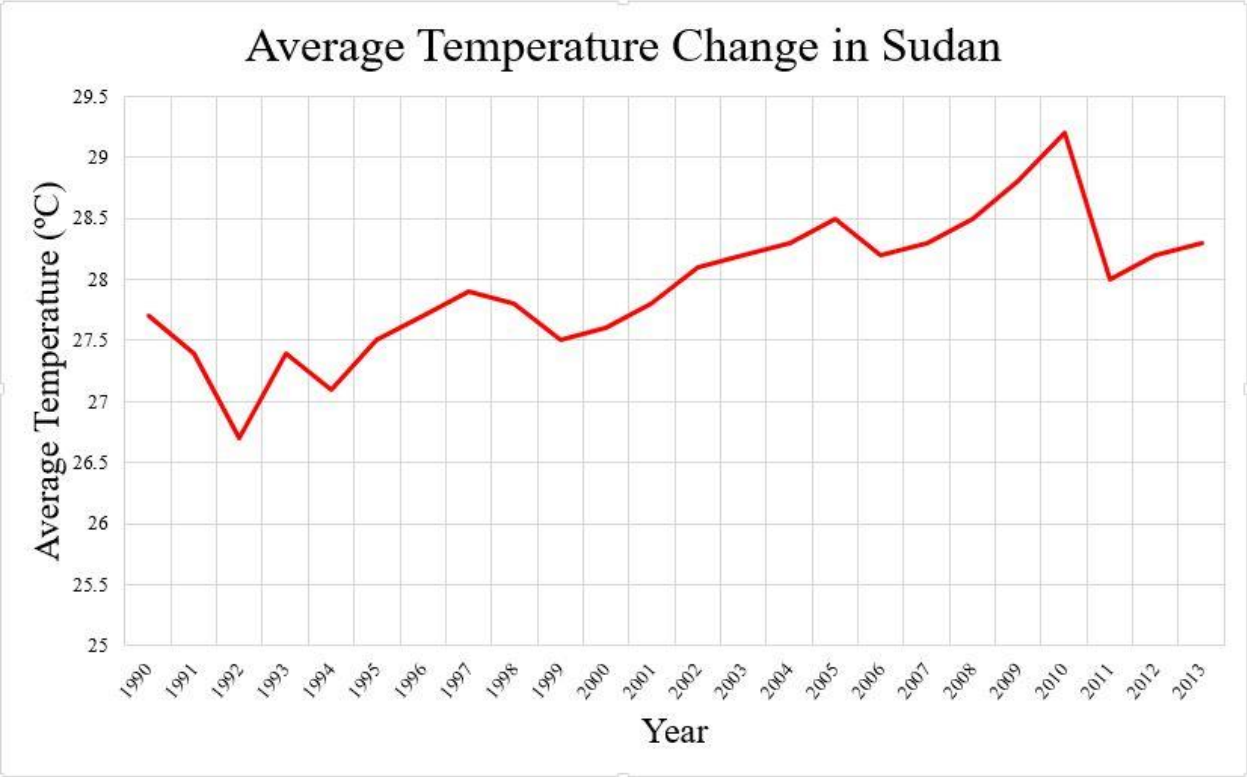

Figure 24: The average temperature change in Sudan from 1990 to 2013.

4.3.3 Precipitation

Figure 25 shows the precipitation in Sudan from 1990 to 2013. According to the figure, 1990 had the lowest participation of rainfall with 310.1 (mm). However, 2007 had the highest amount of precipitation with 498.6 (mm). From 2000 to 2013, there was a considerable variation in rainfall. From 2000 to 2002, precipitation dropped from 427.4 (mm) to 393.1 (mm). However, it increased rapidly in 2003. From 2004 to 2007, precipitation rose from 367.7 (mm) to 498.6 (mm), but it reduced quickly over the following years to be 346.3 (mm) in 2009. Similarly, the expansion of the desert increased from 2000 to 2009. From 2011 to 2013 precipitation increased gradually from 401.5 (mm) to 444.2 (mm). Correspondingly, the desert expansion decreased

during the same period. The expansion of the desert has a strong relationship with the precipitation. Low rainfall increases the chances of the dry lands to convert into desert.

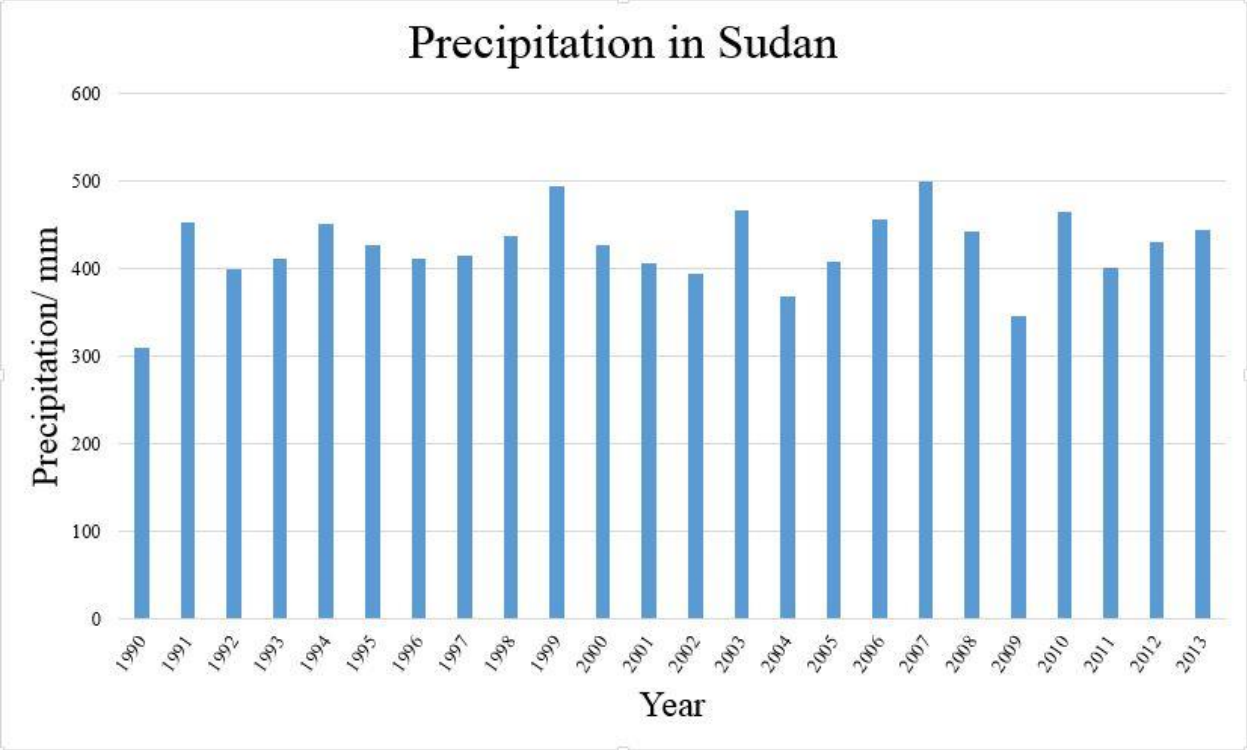

Figure 25: The precipitation dynamics in Sudan from 1990 to 2013.

CHAPTER 5

DISCUSSION AND CONCLUSION

This study attempted to answer three research questions to evaluate the expansion, causes, and the impact of desertification in Sudan. This chapter consists of three concepts: the desert expansion over time and space, the factors of the desert expansion, and the impact of desertification on the environment and vegetation condition.

5.1 The Desert area in Sudan Over Time and Space

The first research question: *How has the desert area in Sudan developed spatially and temporally?*

Two kinds of satellite images were used to evaluate the magnitude of the desert over time and space. The Landsat and MODIS images were classified using ANN and SMA methods. The results using ANN led to more accurate and reasonable classification maps based on the accuracy assessment and because the map demonstrated a close agreement with prior research (Eltoum et al., 2015). In ANN, three classes were identified from the study area: vegetation, desert, and rock. The image classification showed that during the last 14 years vegetation has decreased and converted to desert. It also indicated that the direction of the desert expansion was towards the south and southwest. In 2000, the magnitude of the desert and vegetation was almost equal, 46.51 % and 46.01 %, respectively. Rock had the smallest percentage at 7.42 %. In 2009, the percentages of the desert and rock area increased to 55.08 % and 8.03 %, respectively, while vegetation percentage had declined to 36.61 %. In 2014, desert and vegetation percentage changed to 58.28 % and 40.69%, while rock reduced to 1.02 %. From 2009 to 2014 the desert decreased by 1.49 %. During the same period the Forest National Corporation (FNC) and the

Office of the United Nations High Commissioner for Refugees (UNHCR) made plans to combat desertification and to re-green Darfur and Kordofan states. UNHCR has planted about 19 million trees to re-green Sudan landscape. NFC and the Sudanese government provided plants and seeds to encouraged citizens to plant surrounding their houses in Darfur state.

The accuracy assessment of the classified images was good despite the omission and commission errors. The classified map produced from the 2014 Landsat data demonstrated an excellent overall classification accuracy and kappa statistic of 86.47 % and 78.37 % respectively. Due to the lack of available data, the 2014 Landsat image was used as a reference map to carry out the accuracy assessment of all of the classified maps of MODIS data. Thus, the accuracy assessment of ANN derived maps for the years of 2000 and 2009 are associated with uncertainties. Three error matrices were produced for three years 2000, 2009, and 2014 (Section 4.1.3). The overall classification accuracy for 2000, 2009, and 2014 classified map was 79.52 %, 81.90 %, and 85.76 % respectively. The accuracy assessments of SMA derived maps were only produced for 2014, and it shows an acceptable agreement with an overall classification accuracy of 76.42 %.

5.2 The Major Factors of the Desert Expansion

The second research question: *What are the major factors that have significantly affected the spatial and temporal expansion of the desert areas in Sudan?*

Many factors might have affected the expansion of desert areas in Sudan. However, because of data limitations, in this study only temperature change, precipitation change and population growth were considered as the major factors that drove the desert expansion. The changes in temperature and precipitation directly and indirectly affected land degradation,

particularly through their influence on vegetation and soil condition. Due to the increase of greenhouse gas emissions during the 21st Century, the average temperature has increased by 2 ºC to 5 ºC in dryland (http://www.unesco.org/). In 2000, the average temperature was 27.6 ºC. However, in 2013, the average temperature was 28.3 ºC. The temperature increase may influenced particular types of plants such as Sorghum crop. For example, if the temperatures of increase above 30 ºC there will be damage in the growth of the Sorghum as well as other vegetation species that favored in the cool season. High temperature increases the rate of evapotranspiration, leading to low soil humidity and thus increasing drought conditions. Consequently, the increased drought conditions may lead to desertification of land.

Another factor that may influence the expansion of desert area in Sudan is rainfall variation. Rainfall variability plays a significant role in dryland climates. If the precipitation is less than evapotranspiration, plants will not have suitable conditions to grow. Sudan has a high fluctuation in the spatial and temporal distribution of rainfall with most of rainfall lower than the required minimum amount to support plant growth. These vegetation decreases are linked to land desertification. Desertification in turn leads to disastrous consequences such as famine because of reduced availability of food crops. In 1931, my study area experienced great famine as a result of low precipitation, high temperatures and soil degradation (Eltoum et al., 2015). If no significant measures are carried out, this process could take place again.

Population growth was one of the major factors that is led to desert expansion. As the total population increases, the pressure on natural resources, such as vegetation and water, also increases. More land is needed for shelter, cultivation, grazing, and wood gathering and this comes at the expense of vegetation. Sudan's population has increased due to the high birthrate and migrations. The high migration of people from South Sudan as well as city dwellers has led

to population growth in the study area. Migration to the desert region was caused by the civil war in South Sudan and the high cost of living expenses in the urban area such as Khartoum. In 2000, the total population in Sudan was about 28.07 million. However, in 2014, the population was approximately 39.35 million. As population increases, anthropogenic activities such as overgrazing and over-cultivation increase. Soil degradation will be the result. The growth of population in the arid, semi-arid, or sub-humid regions increases demands on the natural ecosystems and thus causes severe soil degradation, which can lead to desertification in these regions (Mengistu, 2008).

5.3 The Impact of Desertification

The Third research question: *What are the impacts of desertification on the environment and vegetation conditions in the past and present?*

Desertification had a negative impact on the environment and vegetation in Sudan over the past 14 years. In dry areas, the deterioration of vegetation cover influences the topsoil temperature and air humidity and therefore, affects the movement of atmospheric masses and rainfall. Additionally, loosened soil cover can easily be eroded by strong winds, increasing the frequency of desert storms. Loosened soils can bury certain types of vegetation like creeping plants, stem tubers, and root tubers. Nutrients in the soil can also be removed by wind or water and salt can build up in the soil, leading to unsuitable conditions for vegetation growth. Desertification also has an impact on carbon exchange. In dry land areas, as the deterioration of vegetation increases, the amount of carbon that is store in the vegetation and soil decreases. This leads to increased atmospheric carbon, which blocks heat from escaping and leads to high temperature and consequently, global warming. Desertification also reduces the biodiversity due

to decreased vegetation species and animal habitat. Furthermore, desertification also negatively impacts water reserves such as rivers and groundwater tables (Manal, 2007).

5.4 Conclusions

GIS and remote sensing technology has been widely used to evaluate and monitor the process of desertification in Sudan. In this study MODIS and Landsat data with ANN and SMA techniques were used to map and analyze the desertification process. Population and climate data such as temperature and rainfall were examined to understand possible dynamics and causes of desertification process for the years 2000, 2009, and 2014. The results indicated a significant decline in the vegetation cover in 2000, 2009, and 2014, which was consistent with those of other studies (Eltoum et al., 2015). Meanwhile, the desert areas have expanded rapidly towards the southern parts of Sudan during the same temporal periods, at the expense of vegetation. Population, temperature, and rainfall are the major factors that have likely enhanced and contributed to the desert expansion. Desertification has a negative influence on the environment and vegetation conditions in Sudan.

5.5 Limitation of the Study

Collection of field observation was not carried out in the study area and only 2014 Landsat data were available. Thus, Landsat data derived results were used as a reference to carry out accuracy assessment of the maps from 2000, 2009, and 2014 MODIS data. Moreover, due to the lack of data, this study only assumed that population growth, temperature and precipitation were the major factors of desert expansion without conducting statistical test to determine the relationship between desert expansion and the major factors.

REFERENCES

Abd El-Kawy, O. R., J. K. Rod, H. A. Ismail, and A. S. Suliman. (2011). Land use and land cover change detection in the western Nile delta of Egypt using remote sensing data. Applied Geography 31, no 2 (2011): 483-494.

Abdi, Omar A., Edinam K. Glover, and Olavi Luukkanen. (1926). Causes and impacts of land degradation and desertification: case study of the Sudan. International Journal of Agriculture and Forestry 3, no 2 (1926): 40-51.

Al-Bakri, J. T., J. C. Taylor, and T. R. Brewer. (2001). Monitoring land use change in the Badia transition zone in Jordan using aerial photography and satellite imagery. The Geographical Journal, 167 no 3 (2001): 248-262.

Anderson, J.R., Hardy, E.T., Roach, J.T., Witmer, R.E. (1976). A Land Use And Land Cover Classification system for Use with Remote Sensor Data. U.S. Geol. Survey prof. Paper (Vol. 964). U.S. Government Printing Office, Washington, DC.

Ares, Jorge, Héctor Del Valle, and Alejandro Bisigato. (2003). Detection of process-related changes in plant patterns at extended spatial scales during early dryland desertification. Global Change Biology 9, no. 11 (2003), 1643-1659.

Ayoub, Ali Taha. (1998). Extent, severity and causative factors of land degradation in the Sudan. Journal of Arid Environments 38, no. 3 (1983): 397-409.

Barth, Hans-Jörg. (1999). Desertification in the eastern province of Saudi Arabia. Journal of arid environments 43, no. 4 (1999): 399-410.

Benkeblia, Noureddine, ed. (2014). Agroecology, Ecosystems, and Sustainability. CRC Press.

Campbell J, B. Wynne R, H. (2011). Introduction to Remote Sensing, A Division of Guilford Publication, Inc.

Chandra. A. M, Ghosh. S. K. (2006). Remote Sensing and Geographical Information System. Alpha Science International LTD.

Congalton, R. G. (1991). A review of assessing the accuracy of classifications of remotely sensed data. Remote Sensing of Environment 37, no. 1(1991): 35–46.

Dewan, Ashraf M., and Yasushi Yamaguchi. (2009). Land use and land cover change in Greater Dhaka, Bangladesh: using remote sensing to promote sustainable urbanization. Applied Geography 29, no. 3 (2009): 390-401.

Dubovyk, Olena, Gunter Menz, Christopher Conrad, Elena Kan, Miriam Machwitz, and Asia Khamzina. (2013). Spatio-temporal analyses of cropland degradation in the irrigated lowlands of Uzbekistan using remote-sensing and logistic regression modeling. Environmental monitoring and assessment 185, no. 6 (2013): 4775-4790.

Elagib, Nadir Ahmed. (2010). Trends in intra-and inter-annual temperature variabilities across Sudan. Ambio 39, no. 5-6 (2010): 413-429.

Eltoum, Mohammed Abdalla, Mohamed Salih Dafalla, and Ibrahim Saeed Ibrahim. (2016). The Role of Ecological Factors in Causing Land Surface Desertification, the Case of Sudan.

Grahami I. H. Kerely and Walter G. Whitford. (2000). Impact of Grazing and Desertification in the Chihuahuan Desert: Plant Communities, Granivores and Granivory. The American Midland Naturalist 144, no. 1 (2000):78-91.

Holcomb, Derrold W. (2001). Imaging radar and archaeological survey: An example from the Gobi Desert of Southern Mongolia. Journal of field archaeology 28 no. 1-2 (2001):131-141.

http://data.worldbank.org/country/sudan Accessed on February 21, 2016. 4:12 P.M

http://www.ncdc.noaa. gov/cdo-web/ Accessed on February 21, 2016. 4:12 P.M

http://www.tradingeconomics.com/ Accessed on February 14, 2016. 2:19 P.M

https://ilri.org/InfoServ/Webpub/fulldocs/Critical/resource.htm Accessed on November 24, 2014. 10:12 P.M

Hu, Guangyin, Zhibao Dong, Junfeng Lu, and Changzhen Yan. (2012). Driving forces responsible for Aeolian desertification in the source region of the Yangtze River from 1975 to 2005. Environmental Earth Sciences 66, no. 1 (2012): 257-263.

Ibrahim, Fouad N. (1978). The Problem of Desertification in the Republic of the Sudan with Special Reference to Northern Darfur Province.

James B, Campbell. (1996). Introduction to Remote Sensing. A Division of Guilford Publication, Inc.

Jensen, J.R., (1996). Introductory Digital Image Processing: A Remote Sensing Perspective, second ed. Prentice Hall, Upper Saddle River, NJ.

Kassas, M. (1995). Desertification: a general review. Journal of Arid Environments 30, no. 2 (1995): 115-128.

Kassas, M., J. Ahmad, and B. Rozanov. (1991). Desertification and drought: an ecological and economic analysis. Desertification Control Bulletin. 20: 19-29.

Kerley, Graham IH, and Walter G. Whitford. (2000). Impact of grazing and desertification in the Chihuahuan Desert: plant communities, granivores and granivory. The American midland naturalist 144, no. 1 (2000): 78-91.

Liu JY (1996) Macro-scale survey and dynamic study of natural resources and environment of china by remote sensing. Sci Technol Press, Beijing (in Chinese).

Liu, Aixia, Jing Wang, Zhengjun Liu, and Jian Wang. (2005). Monitoring desertification in arid and semi-arid areas of China with NOAA-AVHRR and MODIS data. In Geoscience and Remote Sensing Symposium, 2005. IGARSS'05. Vol 4, pp. 2362- 2364. IEEE, 2005.

Mallinis, G. (2008). Object-based classification using QuickBird imagery for delineating forest vegetation polygons in Mediterranean test site. Photogram and Remote Sensing 63, no. 2 (2008): 237-250.

Matthewson, A.P G. B. Shimmield, and D. Kroon. (1995). A 300 kyr High- resolution Aridity Record of the North African Continent. Paleoceanography 10, no. 3(1995): 677- 692.

Mike Hulme. (1996). Recent climatic change in the world's drylands. Geophysical research letters 23, no. 1 (1996): 61-64.

Murai, S. (1996). Remote Sensing Note, second ed. Nihon Printing Co. Ltd., Tokyo. 220–221.

OFDA. (1990). Disaster History, Washington DC, USA.

Oliver, John E., ed (2005). The encyclopedia of world climatology. Springer.

Osman, Yassin Z., and Asaad Y. Shamseldin. (2002). Qualitative rainfall prediction models for central and southern Sudan using El Niño–Southern Oscillation and Indian Ocean sea surface temperature indices. International journal of climatology 22, no. 15 (2002): 1861-1878.

Ouma, G. O., and L. A. Ogallo. (2007). Desertification in Africa.

P. F. Reich, S.T. Numbem, R. A. Almaraz, H. Eswaran. (2001). Land Resource Stresses and Desertification in Africa. Agro- Science. 1-10.

Shahin, Mamdouh. (2007). Water resources and hydrometeorology of the Arab region.

Shalaby, Adel, and Ryutaro Tateishi. (2007). Remote sensing and GIS for mapping and monitoring land cover and land-use changes in the Northwestern coastal zone of Egypt. Applied Geography 27, no. 1 (2007): 28-41.

Swain, Ashok. (1997). Ethiopia, the Sudan, and Egypt: The Nile River Dispute. The Journal of Modern African Studies 35, no. 4 (1997): 675-694.

Tolba, Mostafa Kamal. (1986). Desertification in Africa. Land Use Policy. 3: 260-268.

UNCOD A/CONF 74/36. (1977). Plan of action to stop desertification. Report on the UN Conf . On Desertificaion, Nairobi.

UNCOD A/CONF. (1977). World map of desertification. Doc. of the UN Conference: on Desertification, Nairobi.

UNCOD. (1977). Round-up, Plan of Action and Resolutions. United Nations Conference on Desertification, Nairobi, Kenya. 43 p.

UNEP. (1992). World Adas of Desertification. London: Edward Arnold. pp 69.

Wang, T., C. Z. Yan, X. Song, and J. L. Xie. (2012). Monitoring recent trends in the area of Aeolian Desertified Land Using Landsat Images in China's Xinjiang region. ISPRS Journal of Photogrammetry and Remote Sensing 68 (2012): 184-190.

Wessels, Konrad J., Stephen D. Prince, Mark Carroll, and Johan Malherbe. (2007). Relevance of rangeland degradation in semiarid northeastern South Africa to the nonequilibrium theory. Ecological Applications 17, no. 3 (2007): 815-827.

Worster, D. (1986). The dirty thirties: a study in agricultural capitalism. Great Plains Quarterly (1986): 107-116.

Wu, Qiong, Hong-qing Li, Ru-song Wang, Juergen Paulussen, Yong He, Min Wang, Bi-hui Wang, and Zhen Wang. (2006). Monitoring and predicting land use change in Beijing

using remote sensing and GIS. Landscape and urban planning 78, no. 4 (2006): 78: 322-333.

Xiao, Jieying, Yanjun Shen, Jingfeng Ge, Ryutaro Tateishi, Changyuan Tang, Yanqing Liang, and Zhiying Huang. (2006). Evaluating urban expansion and land use change in Shijiazhuang, China, by using GIS and remote sensing. Landscape and urban planning 75, no. 1 (2006): 69-80.

Xu, Duanyang, Xiangwu Kang, Dongsheng Qiu, Dafang Zhuang, and Jianjun Pan. (2009). Quantitative assessment of desertification using landsat data on a regional scale–a case study in the Ordos plateau, china. Sensors 9, no. 3 (2009): 1738-1753.

Zha, Yong, and Jay Gao. (1997). Characteristics of desertification and its rehabilitation in China. Journal of Arid Environments 37, no. 3 (1997): 419-432.

VITA

Graduate School
Southern Illinois University

Tarig Ail Mohamed

Tarig.mohamed@siu.edu

Future University, Khartoum, Sudan

Bachelors of Science in Information Technology, January 2010

Thesis Title:

MONITORING AND ANALYZING OF DESERTIFICATION TREND IN NORTH SUDAN USING MODIS IMAGES FROM 2000 TO 2014

Major Professor: Dr. Guangxing Wang